International Journal of Bifurcation and Chaos, Vol. 18, No. 11 (2008) 3183–3206

MEMRISTOR OSCILLATORS

MAKOTO ITOH
Department of Information and Communication Engineering,
Fukuoka Institute of Technology,
Fukuoka 811-0295, Japan

LEON O. CHUA
Department of Electrical Engineering and Computer Sciences,
University of California, Berkeley,
Berkeley, CA 94720, USA

Received July 15, 2008; Revised September 18, 2008

The *memristor* has attracted phenomenal worldwide attention since its debut on 1 May 2008 issue of *Nature* in view of its many potential applications, e.g. super-dense nonvolatile computer memory and neural synapses. The Hewlett–Packard memristor is a passive nonlinear two-terminal circuit element that maintains a functional relationship between the time integrals of current and voltage, respectively, viz. *charge* and *flux*. In this paper, we derive several nonlinear oscillators from Chua's oscillators by replacing Chua's diodes with memristors.

Keywords: Memristor; memristive devices; memristive systems; charge; flux; Chua's oscillator; Chua's diode; learning; neurons; synapses; Hodgkin–Huxley; nerve membrane model.

1. Memristors

In a seminal paper [Strukov *et al.*, 2008] which appeared on 1 May 2008 issue of *Nature*, a team led by R. Stanley Williams from the Hewlett–Packard Company announced the fabrication of a nanometer-size solid-state two-terminal device called the *memristor*, a contraction for *memory resistor*, which was postulated in [Chua, 1971; Chua & Kang, 1976]. This passive electronic device has generated unprecedented worldwide interest[1] because of its potential applications [Tour & He, 2008; Johnson, 2008] in the next generation computers and powerful brain-like "neural" computers. One immediate application offers an enabling low-cost technology for *non-volatile* memories[2] where future computers would turn on instantly without the usual "booting time", currently required in all personal computers.

The HP *memristor* shown in Fig. 1 is a passive two-terminal electronic device described by a nonlinear constitutive relation

$$v = M(q)i, \quad \text{or} \quad i = W(\varphi)v, \tag{1}$$

between the device terminal voltage v and terminal current i. The two nonlinear functions $M(q)$ and $W(\varphi)$, called the *memristance* and *memductance*, respectively, are defined by

$$M(q) \triangleq \frac{d\varphi(q)}{dq}, \tag{2}$$

and

$$W(\varphi) \triangleq \frac{dq(\varphi)}{d\varphi}, \tag{3}$$

representing the *slope* of a scalar function $\varphi = \varphi(q)$ and $q = q(\varphi)$, respectively, called the *memristor constitutive relation.*

[1]More than one million Google hits were registered as of June 1, 2008.

[2]The Hewlett–Packard memristor is a tiny nano, passive, two-terminal device requiring no batteries. Memristors characterized by a nonmonotonic constitutive relation are called *active* memristors in this paper because they require a power supply.

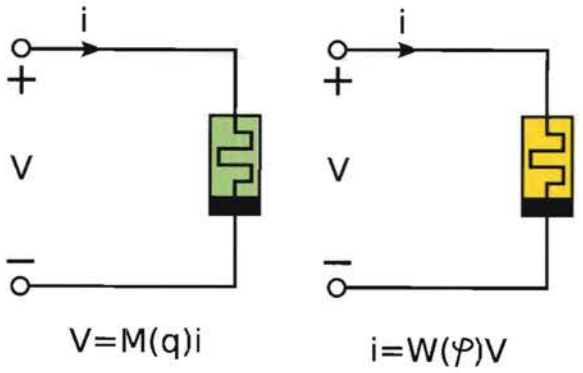

Fig. 1. Charge-controlled memristor (left). Flux-controlled memristor (right).

A memristor characterized by a differentiable $q-\varphi$ (resp. $\varphi-q$) characteristic curve is *passive* if, and only if, its small-signal memristance $M(q)$ (resp. small-signal memductance $W(\varphi)$) is non-negative; i.e.

$$M(q)=\frac{d\varphi(q)}{dq}\geq 0 \quad \left(\text{resp. } W(\varphi)=\frac{dq(\varphi)}{d\varphi}\geq 0\right) \tag{4}$$

(see [Chua, 1971]). In this paper, we assume that the memristor is characterized by the "*monotone-increasing*" and "*piecewise-linear*" nonlinearity shown in Fig. 2, namely,

$$\varphi(q)=bq+0.5(a-b)(|q+1|-|q-1|), \tag{5}$$

or

$$q(\varphi)=d\varphi+0.5(c-d)(|\varphi+1|-|\varphi-1|), \tag{6}$$

where $a,\ b,\ c,\ d>0$. Consequently, the memristance $M(q)$ and the memductance $W(\varphi)$ in Fig. 2 are defined by

$$M(q)=\frac{d\phi(q)}{dq}=\begin{cases}a, & |q|<1,\\ b, & |q|>1,\end{cases} \tag{7}$$

and

$$W(\varphi)=\frac{dq(\varphi)}{d\varphi}=\begin{cases}c, & |w|<1,\\ d, & |w|>1,\end{cases} \tag{8}$$

respectively. Since the instantaneous power dissipated by the above memristor is given by

$$p(t)=M\big(q(t)\big)i(t)^2\geq 0, \tag{9}$$

or

$$p(t)=W\big(\varphi(t)\big)v(t)^2\geq 0, \tag{10}$$

the energy flow into the memristor from time t_0 to t satisfies

$$\int_{t_0}^{t}p(\tau)d\tau\geq 0, \tag{11}$$

for all $t\geq t_0$. Thus, the memristor constitutive relation in Fig. 2 is *passive*.

Consider next the two-terminal circuit in Fig. 3, which consists of a *negative* resistance[3] (or a negative conductance) and a passive memristor. If the two-terminal circuit has a flux-controlled

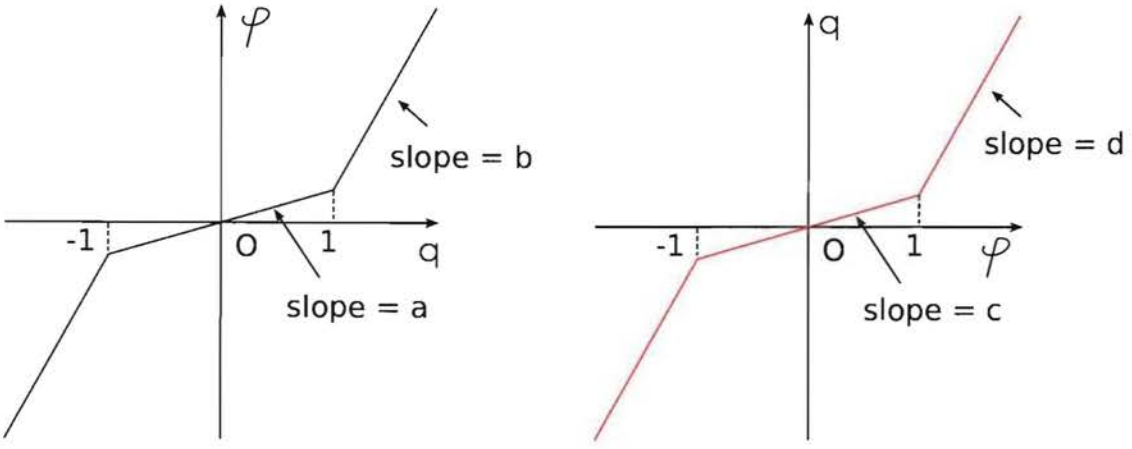

Fig. 2. The constitutive relation of a monotone-increasing piecewise-linear memristor: Charge-controlled memristor (left). Flux-controlled memristor (right).

[3]The negative resistance or conductance can be realized by a standard op amp circuit, powered by batteries.

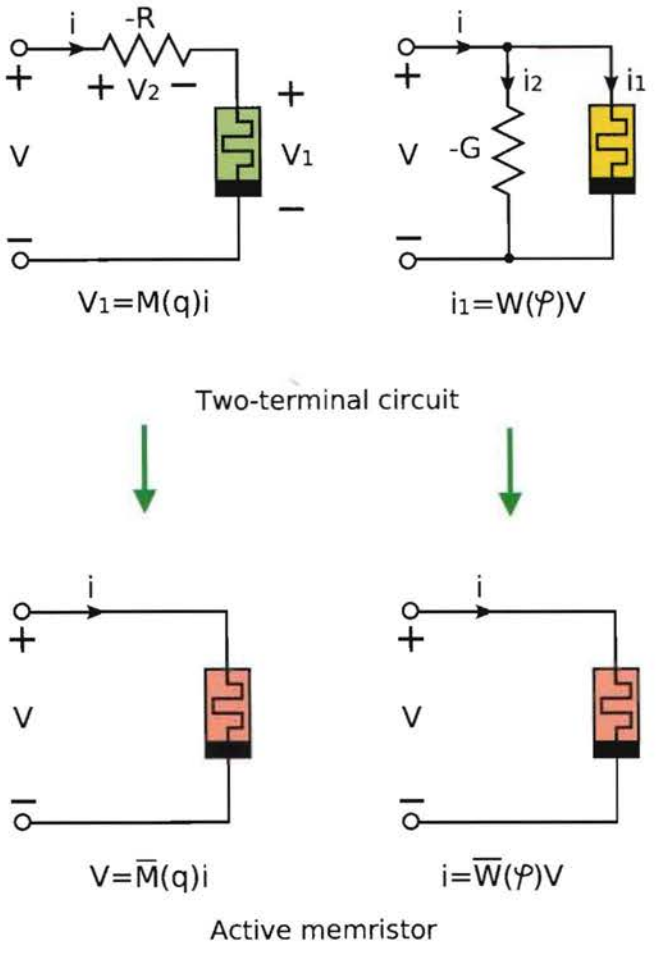

Fig. 3. Two-terminal circuit which consists of a memristor and a negative conductance $-G$ (or a resistance $-R$).

memristor, we obtain the following $\varphi - q$ curve

$$\begin{aligned} q(\varphi) &= \int i(\tau)d\tau \\ &= \int (i_1(\tau) + i_2(\tau))d\tau \\ &= \int (W(\varphi)v - Gv)d\tau \\ &= \int (W(\varphi) - G)vd\tau \\ &= \int (W(\varphi) - G)d\varphi \left(\frac{d\varphi}{d\tau} = v\right) \\ &= d\varphi + 0.5(c-d)(|\varphi+1| - |\varphi-1|) - G\varphi \\ &= (d-G)\varphi + 0.5(c-d)(|\varphi+1| - |\varphi-1|), \end{aligned} \tag{12}$$

where we assumed that $q(\varphi)$ is a continuous function satisfying $q(0) = 0$ and $G > 0$. Thus, the small signal memductance $\overline{W}(\varphi)$ of this two-terminal circuit is given by

$$\overline{W}(\varphi) = \frac{dq(\varphi)}{d\varphi} = \begin{cases} c - G, & |w| < 1, \\ d - G, & |w| > 1. \end{cases} \tag{13}$$

If $c - G < 0$ or $d - G < 0$, then the instantaneous power does not satisfy

$$p(t) = \overline{W}(\varphi(t))v(t)^2 \geq 0, \tag{14}$$

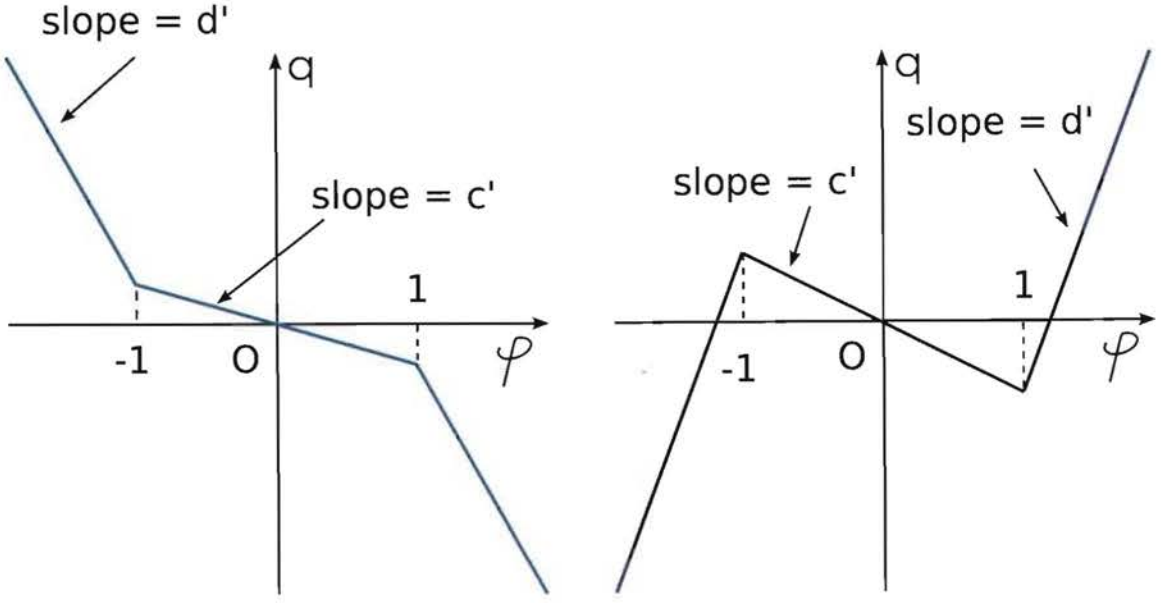

Fig. 4. $\varphi - q$ characteristic of the two-terminal circuit.

for all $t > 0$. In this case, there exists $\varphi(t_0) = \varphi_0$ and

$$\int_{t_0}^{t} p(\tau)d\tau < 0, \tag{15}$$

for all $t \in (t_0, t_1)$. Thus, the two-terminal circuit in Fig. 3 can be designed to become an *active* device, and can be regarded as an "*active memristor*". We illustrate two kinds of characteristic curves in Fig. 4. Similar characteristic curves can be obtained for charge-controlled memristors. In this paper, we design several nonlinear oscillators using active or passive memristors.

2. Circuit Laws

In this section, we review some basic laws for electrical circuits. Recall first the following *principles of conservation of charge and flux* [Chua, 1969]:

- Charge and flux can neither be created nor destroyed. The quantity of charge and flux is always conserved.

We can restate this principle as follows:

- Charge q and voltage v_C across a capacitor cannot change instantaneously.
- Flux φ and current i_L in an inductor cannot change instantaneously.

Applying this principle to the circuit, we can obtain a relation between the two fundamental circuit variables: the "*charge*" and the "*flux*". However, we usually use the other fundamental circuit variables, namely the "*voltage*" and the "*current*" by applying the following *Kirchhoff's circuit laws* [Chua, 1969]:

- The algebraic sum of all the currents i_m flowing into the node is zero:

$$\sum_m i_m = 0. \tag{16}$$

- The algebraic sum of branch voltages v_n around any closed circuit is zero:

$$\sum_n v_n = 0. \tag{17}$$

They are a pair of laws that result from the conservation of charge and energy in electrical circuits. If we apply the Kirchhoff's circuit laws to a memristive circuit, we need the *four fundamental circuit variables*, namely the voltage, current, charge, and flux to describe their dynamics, because the relation between current i and voltage v of the memristor is defined by Eq. (1).

If we integrate the Kirchhoff's circuit laws with respect to time t, we would obtain the relation on the conservation of charge and flux:

$$\sum_m q_m = 0, \tag{18}$$

and

$$\sum_n \varphi_n = 0. \tag{19}$$

where q_m and φ_n are defined by

$$q_m = \int_{-\infty}^{t} i_m dt, \tag{20}$$

and

$$\varphi_n = \int_{-\infty}^{t} v_n dt, \tag{21}$$

respectively.

The relationship between voltage v and current i for the four fundamental circuit elements is given by

- Capacitor

$$C\frac{dv}{dt} = i \tag{22}$$

- Inductor

$$L\frac{di}{dt} = v \tag{23}$$

- Resistor

$$v = Ri \tag{24}$$

- Memristor

$$v = M(q)i \quad (\text{or} \quad i = W(\varphi)) \tag{25}$$

Using these relations and the Kirchhoff's circuit laws, we can describe the dynamics of electrical circuits.

Integrating Eqs. (22)–(25) with respect to time t, we obtain the following equations:

- Capacitor

$$q = Cv \tag{26}$$

- Inductor

$$\varphi = Li \tag{27}$$

- Resistor

$$\varphi = Rq \tag{28}$$

- Memristor

$$\varphi = \int M(q)dq \quad \left(\text{or} \quad q = \int W(\varphi)d\varphi\right) \quad (29)$$

where $q = \int_{-\infty}^{t} idt$ and $\varphi = \int_{-\infty}^{t} vdt$. They provide the relationship between Eqs. (16)–(17) and Eqs. (18)–(19).

3. Memristor-Based Canonical Oscillators

Chua's circuit in Fig. 5 is the simplest electronic circuit exhibiting chaotic behavior [Madan, 1993]. It is well known that the *canonical Chua's oscillator* [Chua & Lin, 1990] in Fig. 6 also has a chaotic attractor. In this section, we design a nonlinear oscillator by replacing the "*Chua's diode*" in the canonical Chua's oscillator with a memristor characterized by a "*monotone-increasing*" and "*piecewise-linear*" nonlinearity.

3.1. *A fourth-order canonical memristor oscillator*

Consider the canonical Chua's oscillator in Fig. 6. If we replace the Chua's diode in Fig. 6 with a flux-controlled memristor, we would obtain the circuit of Fig. 7. Its *dual circuit*[4] can be easily obtained by using a charge-controlled memristor (see Fig. 8).

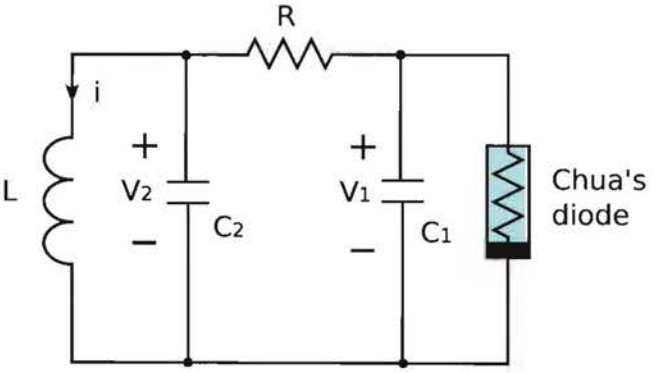

Fig. 5. Chua's circuit.

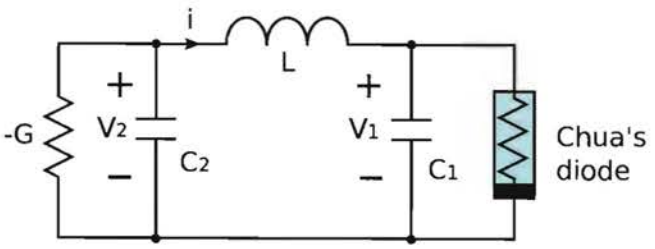

Fig. 6. Canonical Chua's oscillator.

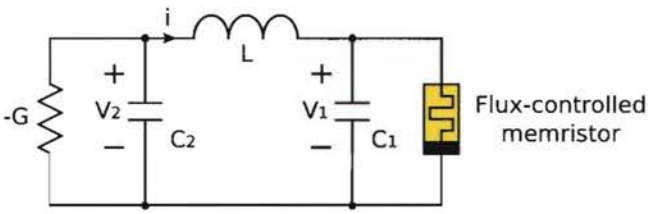

Fig. 7. Canonical Chua's oscillator with a flux-controlled memristor.

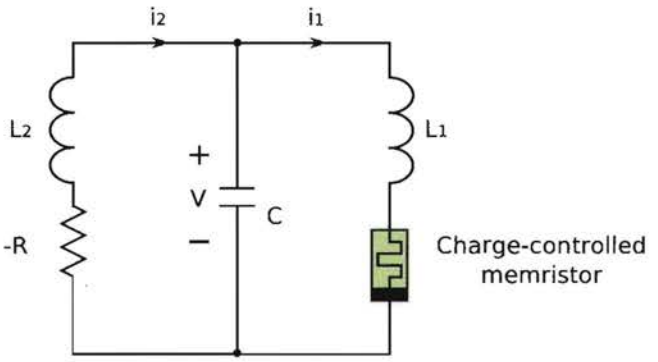

Fig. 8. Dual circuit with a charge-controlled memristor.

Applying Kirchhoff's circuit laws to the nodes A, B and the loop C of the circuit in Fig. 9, we obtain

$$\left.\begin{aligned} i_1 &= i_3 - i, \\ v_3 &= v_2 - v_1, \\ i_2 &= -i_3 + i_4. \end{aligned}\right\} \quad (30)$$

Integrating Eq. (30) with respect to time t, we get a set of equations which define the relation among two fundamental circuit variables, namely, the charge

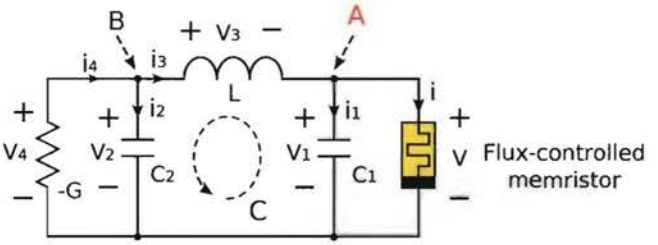

Fig. 9. Currents i_j, voltages v_j, nodes A, B, and loop C are indicated.

[4]A pair of circuits N and N' are dual if the equations of the two circuits are identical, after a trivial change of symbols. For more details, see [Chua, 1969].

and the flux:

$$\left.\begin{aligned} q_1 &= q_3 - q(\varphi), \\ \varphi_3 &= \varphi_2 - \varphi_1, \\ q_2 &= -q_3 + q_4, \end{aligned}\right\} \tag{31}$$

where

$$\left.\begin{aligned} q_1 &\triangleq \int_{-\infty}^{t} i_1(t)dt, \\ q_2 &\triangleq \int_{-\infty}^{t} i_2(t)dt, \\ q_3 &\triangleq \int_{-\infty}^{t} i_3(t)dt, \\ q_4 &\triangleq \int_{-\infty}^{t} i_4(t)dt, \\ q &\triangleq \int_{-\infty}^{t} i(t)dt, \end{aligned}\right\} \quad \left.\begin{aligned} \varphi_1 &\triangleq \int_{-\infty}^{t} v_1(t)dt, \\ \varphi_2 &\triangleq \int_{-\infty}^{t} v_2(t)dt, \\ \varphi_3 &\triangleq \int_{-\infty}^{t} v_3(t)dt, \\ \varphi &\triangleq \int_{-\infty}^{t} v(t)dt = \varphi_1. \end{aligned}\right\} \tag{32}$$

Here, the symbols q_1, q_2, q_3, q_4 and q denote the charge of the capacitors C_1, C_2, the inductor L, the conductance $-G$, and the memristor, respectively, and the symbols $\varphi_1, \varphi_2, \varphi_3$ and φ denote the flux of the capacitors C_1, C_2, the inductor L, and the memristor, respectively. The $\varphi - q$ characteristic curve of the memristor is given by

$$q(\varphi) = b\varphi + 0.5(a-b)(|\varphi+1| - |\varphi-1|). \tag{33}$$

Solving Eq. (31) for $(q_3,\ q_4,\ \varphi_1,\ \varphi_2)$, we get

$$\left.\begin{aligned} q_3 &= q_1 + q(\varphi), \\ q_4 &= q_1 + q_2 + q(\varphi), \\ \varphi_1 &= \varphi, \\ \varphi_2 &= \varphi + \varphi_3. \end{aligned}\right\} \tag{34}$$

Thus, $(q_1, q_2, \varphi, \varphi_3)$ can be chosen to be the independent variables, namely, the charge of the capacitors C_1, C_2, and the flux of the inductor L and the memristor, respectively.

From Eq. (30) (or differentiating Eq. (31) with respect to time t), we obtain a set of four first-order differential equations, which define the relation among the four circuit variables (v_1, v_2, i_3, φ):

$$\left.\begin{aligned} C_1\frac{dv_1}{dt} &= i_3 - W(\varphi)v_1, \\ L\frac{di_3}{dt} &= v_2 - v_1, \\ C_2\frac{dv_2}{dt} &= -i_3 + Gv_2, \\ \frac{d\varphi}{dt} &= v_1, \end{aligned}\right\} \tag{35}$$

where

$$\left.\begin{aligned} \frac{dq_1}{dt} &= i_1 = C_1\frac{dv_1}{dt}, \\ \frac{dq_2}{dt} &= i_2 = C_2\frac{dv_2}{dt}, \\ \frac{dq_3}{dt} &= i_3, \\ \frac{dq_4}{dt} &= i_4 = Gv_2, \end{aligned}\right\} \quad \left.\begin{aligned} \frac{d\varphi_1}{dt} &= v_1, \\ \frac{d\varphi_2}{dt} &= v_2, \\ \frac{d\varphi_3}{dt} &= v_3 = L\frac{di_3}{dt}, \\ W(\varphi) &= \frac{dq(\varphi)}{d\varphi}. \end{aligned}\right\} \tag{36}$$

Note that the two kinds of independent variables are related by

$$\boxed{\begin{array}{c} (q_1,\ q_2,\ \varphi,\ \varphi_3) \quad \longleftrightarrow \quad (v_1,\ v_2,\ \varphi,\ i_3) \\ q_1 = C_1v_1,\ q_2 = C_2v_2,\ \varphi_3 = Li_3 \end{array}} \tag{37}$$

Thus, Eq. (35) can be recast into the following set of differential equations using only charge and flux as variables:

$$\left.\begin{aligned} \frac{dq_1}{dt} &= \frac{\varphi_3}{L} - \frac{W(\varphi)q_1}{C_1}, \quad \frac{d\varphi_3}{dt} = \frac{q_2}{C_2} - \frac{q_1}{C_1}, \\ \frac{dq_2}{dt} &= -\frac{\varphi_3}{L} + \frac{Gq_2}{C_2}, \quad \frac{d\varphi}{dt} = \frac{q_1}{C_1}. \end{aligned}\right\} \tag{38}$$

We next study the behavior of this circuit. Equation (35) can be transformed into the form

$$\left.\begin{aligned} \frac{dx}{dt} &= \alpha\big(y - W(w)x\big), \\ \frac{dy}{dt} &= z - x, \\ \frac{dz}{dt} &= -\beta y + \gamma z, \\ \frac{dw}{dt} &= x, \end{aligned}\right\} \tag{39}$$

where $x = v_1$, $y = i_3$, $z = v_2$, $w = \varphi$, $\alpha = 1/C_1$, $\beta = 1/C_2$, $\gamma = G/C_2$, $L = 1$, and the piecewise-linear functions $q(w)$ and $W(w)$ are given by

$$\left.\begin{aligned} q(w) &= bw + 0.5(a-b)(|w+1| - |w-1|), \\ W(w) &= \frac{dq(w)}{dw} = \begin{cases} a, & |w| < 1, \\ b, & |w| > 1, \end{cases} \end{aligned}\right\} \tag{40}$$

respectively, where $a, b > 0$. Note that the uniqueness of solutions for Eq. (39) cannot be guaranteed since $W(w)$ is discontinuous if $a \neq b$. If we set $\alpha = 4$, $\beta = 1$, $\gamma = 0.65$, $a = 0.2$, and $b = 10$, our computer simulation[5] shows that Eq. (39) has a chaotic attractor as shown in Fig. 10. By calculating the Lyapunov exponents from sampled time series, we found that this chaotic attractor has one positive

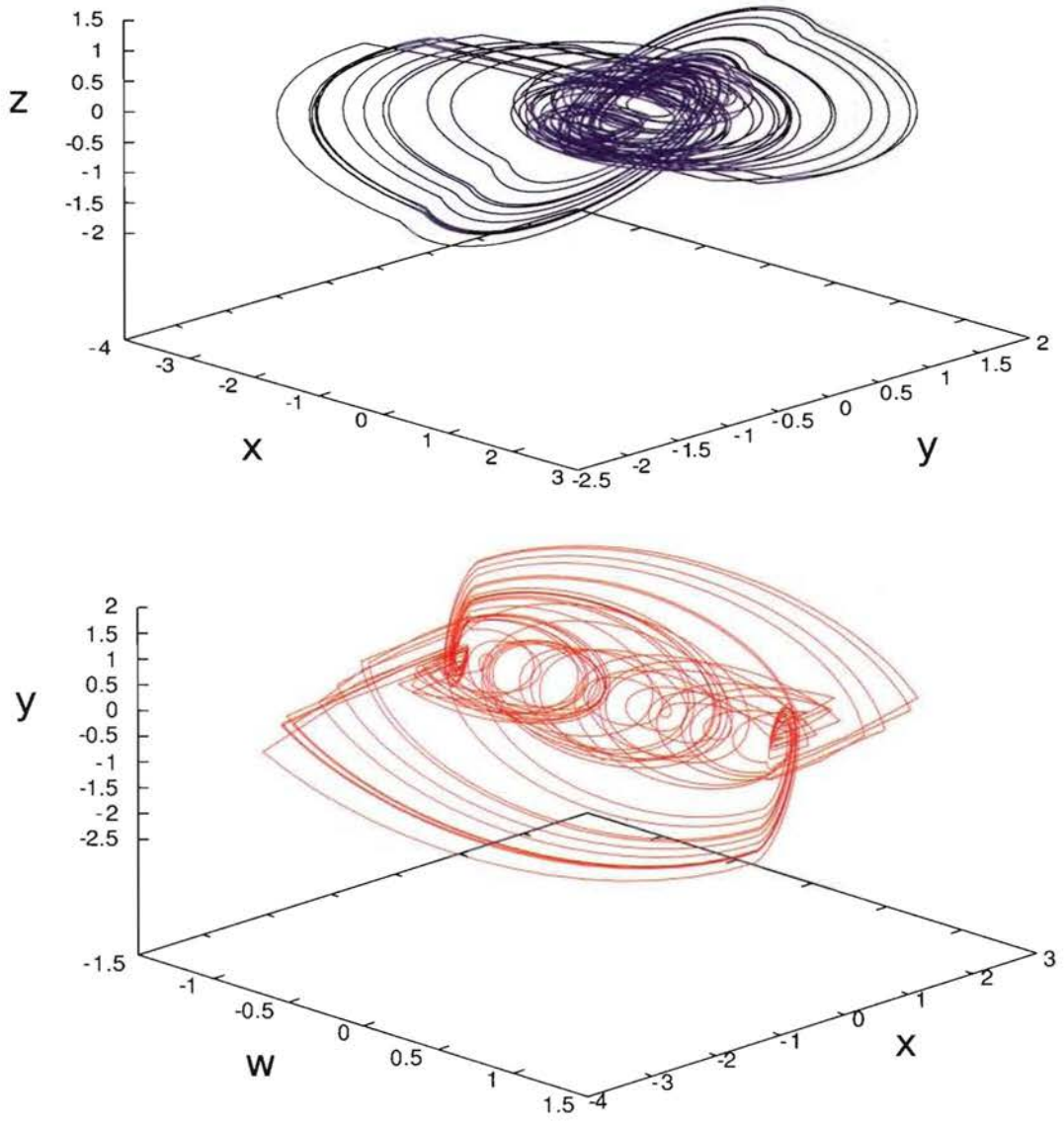

Fig. 10. Chaotic attractor of the canonical Chua's oscillator with a flux-controlled memristor.

[5]We used the *fourth-order Runge-Kutta method* for integrating the differential equations.

Lyapunov exponent $\lambda_1 \approx 0.27$.[6] Furthermore, the divergence of the vector field

$$\begin{aligned}\operatorname{div}(X) &= -\alpha W(w) + \gamma \\ &= -4W(w) + 0.65 \\ &= \begin{cases} -0.15, & |w| < 1, \\ -39.35, & |w| > 1, \end{cases}\end{aligned} \tag{41}$$

is negative. It follows that the Lebesgue measure of this chaotic attractor is zero, and at least one Lyapunov exponent must be negative.[7]

The equilibrium state of Eq. (39) is given by set $A = \{(x, y, z, w) | x = y = z = 0,\ w = constant.\}$, which corresponds to the w-axis. The Jacobian matrix D at this equilibrium set is given by

$$D = \begin{bmatrix} -\alpha W(w) & \alpha & 0 & 0 \\ -1 & 0 & 1 & 0 \\ 0 & -\beta & \gamma & 0 \\ 1 & 0 & 0 & 0 \end{bmatrix}, \tag{42}$$

and its characteristic equation is given by

$$\begin{aligned}&\rho^4 + (\alpha W(w) - \gamma)\rho^3 + (\beta + \alpha - \alpha\gamma W(w))\rho^2 \\ &\quad + \alpha(\beta W(w) - \gamma)\rho = 0.\end{aligned} \tag{43}$$

The four eigenvalues ρ_i $(i = 1, 2, 3, 4)$ of the equilibrium state $(0, 0, 0, w)$ can be written as

$$\left.\begin{aligned} &\rho_{1,2} \approx -0.267093 \pm i\,2.148, \quad \rho_3 \approx 0.384186, \quad \rho_4 = 0, \quad \text{for } |w| < 1, \\ &\rho_{1,2} \approx 0.274905 \pm i\,0.928318, \quad \rho_3 \approx -39.8998, \quad \rho_4 = 0, \quad \text{for } |w| > 1. \end{aligned}\right\} \tag{44}$$

Thus, they are characterized by an unstable saddle-focus except for the zero eigenvalue. Furthermore, Eq. (39) can be transformed into the form

$$\begin{aligned}&\frac{d^3z}{dt^3} + (\alpha W(w) - \gamma)\frac{d^2z}{dt^2} + (\beta + \alpha - \alpha\gamma W(w))\frac{dz}{dt} \\ &\quad + \alpha(\beta W(w) - \gamma)z = 0.\end{aligned} \tag{45}$$

If we substitute

$$u(t) = \int_0^t z(t)dt + u_0, \tag{46}$$

into Eq. (45), we would obtain a fourth-order differential equation in the variable u; namely,

$$\begin{aligned}&\frac{d^4u}{dt^4} + (\alpha W(w) - \gamma)\frac{d^3u}{dt^3} + (\beta + \alpha - \alpha\gamma W(w))\frac{d^2u}{dt^2} \\ &\quad + \alpha(\beta W(w) - \gamma)\frac{du}{dt} = 0,\end{aligned} \tag{47}$$

where

$$w(t) = \frac{\beta u - \gamma\dfrac{du}{dt} + \dfrac{d^2u}{dt^2}}{\beta} + w_0. \tag{48}$$

Here, u_0 and w_0 are constants. Thus, its characteristic equation also has a zero eigenvalue.

Consider next the fourth-order oscillator in Fig. 11 obtained by removing a resistor from the circuit of Fig. 7. The circuit equation can be written as

$$\left.\begin{aligned} C_1\frac{dv_1}{dt} &= i_3 - W(\varphi)v_1, \\ L\frac{di_3}{dt} &= v_2 - v_1, \\ C_2\frac{dv_2}{dt} &= -i_3, \\ \frac{d\varphi}{dt} &= v_1, \end{aligned}\right\} \tag{49}$$

Equation (35) can be transformed into the form

$$\left.\begin{aligned} \frac{dx}{dt} &= \alpha\big(y - W(w)x\big), \\ \frac{dy}{dt} &= -\xi(x + z), \\ \frac{dz}{dt} &= \beta y, \\ \frac{dw}{dt} &= x, \end{aligned}\right\} \tag{50}$$

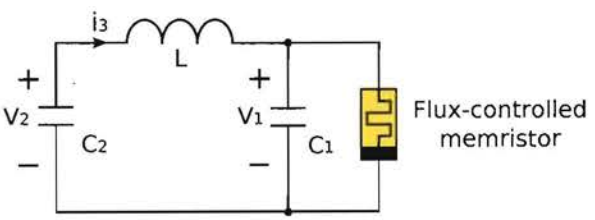

Fig. 11. A fourth-order oscillator with a flux-controlled memristor.

[6]We used the software package *MATDS* [Govorukhin, 2004] to calculate the Lyapunov exponents.

[7]Note that if the system is a flow, one Lyapunov exponent is always zero, which corresponds to the direction of the flow.

where $x = v_1$, $y = i_3$, $z = -v_2$, $w = \varphi$, $\alpha = 1/C_1$, $\beta = 1/C_2$, $\xi = 1/L$, and the piecewise-linear functions $q(w)$ and $W(w)$ are given by

$$\left.\begin{aligned} q(w) &= bw + 0.5(a-b)(|w+1| - |w-1|), \\ W(w) &= \frac{dq(w)}{dw} = \begin{cases} a, & |w| < 1, \\ b, & |w| > 1. \end{cases} \end{aligned}\right\} \quad (51)$$

From Eq. (50), we obtain

$$\frac{d}{dt}\left\{\frac{1}{2}\left(\frac{x^2}{\alpha} + \frac{y^2}{\xi} + \frac{z^2}{\beta}\right)\right\} = -W(w)x^2 \leq 0, \quad (52)$$

assuming $a > 0$ and $b > 0$. In this case, the equilibrium state $A = \{(x, y, z, w) | x = y = z = 0,\ w = \text{constant}\}$ (i.e. the w-axis) is globally asymptotically stable, and Eq. (50) does not have a chaotic attractor. However, if we set $\alpha = 4.2$, $\beta = -20$, $\xi = -1$, $a = -2$ and $b = 9$, our computer simulation of Eq. (50) gives a chaotic attractor in Fig. 12. By calculating the Lyapunov exponents from sampled time series, we found that this chaotic attractor has a positive Lyapunov exponent $\lambda_1 \approx 0.050$. In this case, the capacitance C_2 and the inductance L are both *negative* (active) and the memristor is *active* as shown in Fig. 13 (see [Barboza & Chua, 2008]).

The Jacobian matrix D at the equilibrium set is given by

$$D = \begin{bmatrix} -\alpha W(w) & \alpha & 0 & 0 \\ -\xi & 0 & -\xi & 0 \\ 0 & \beta & 0 & 0 \\ 1 & 0 & 0 & 0 \end{bmatrix}, \quad (53)$$

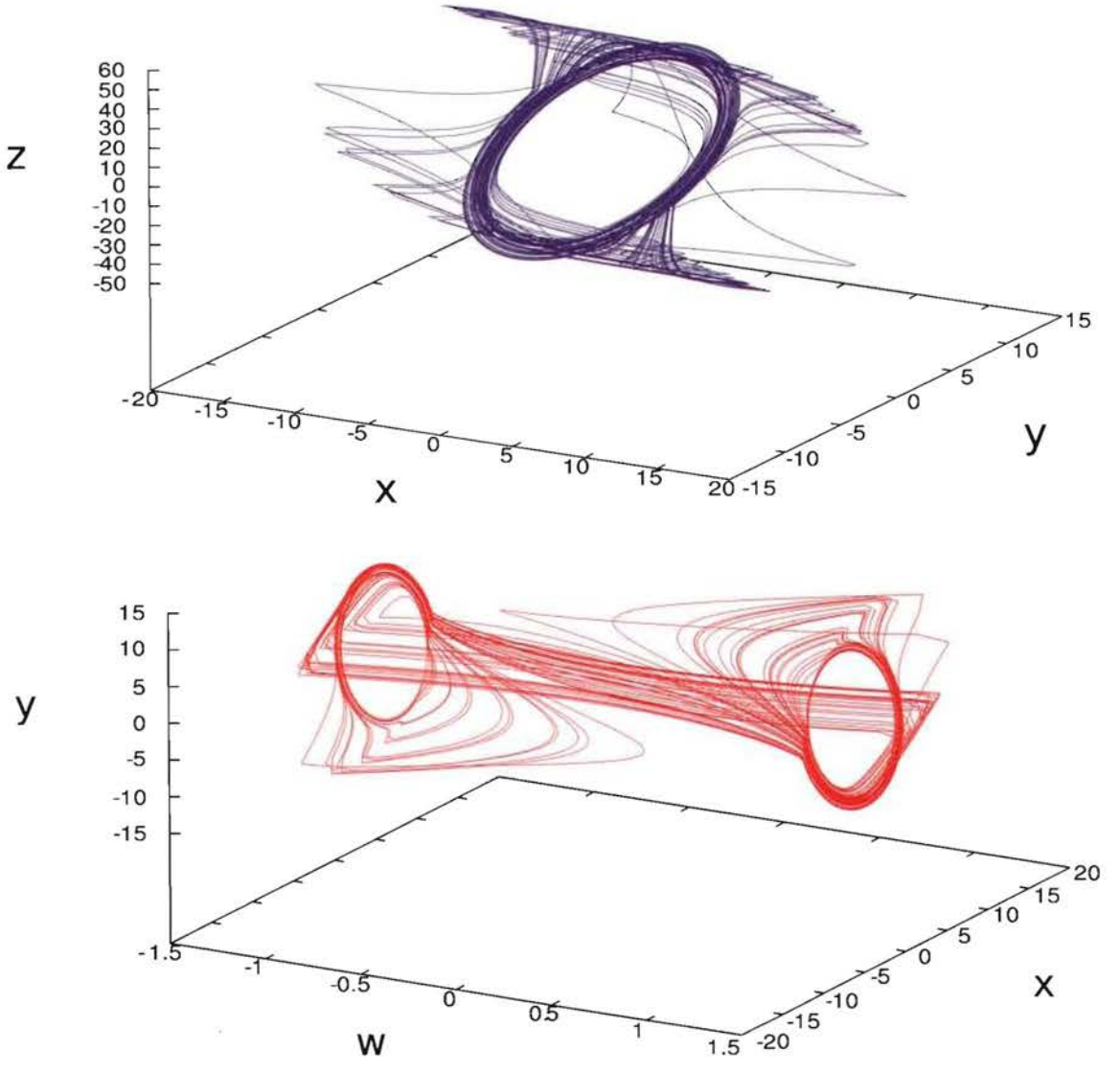

Fig. 12. Chaotic attractor of the fourth-order oscillator with active elements ($a = -1, b = 5$).

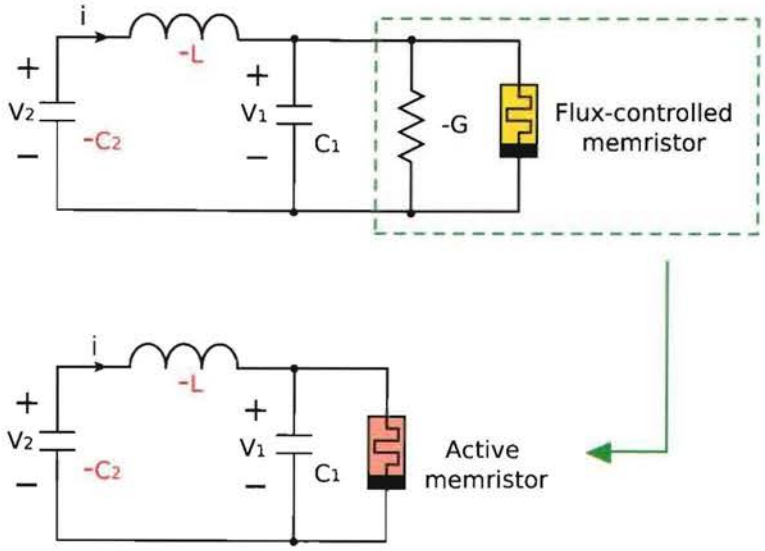

Fig. 13. A four-element fourth-order oscillator with three *active* elements, one linear capacitor, one linear inductor, and a memristor.

and its characteristic equation is given by

$$\rho^4 + \alpha W(w)\rho^3 + (\alpha+\beta)\xi\rho^2 + \alpha\beta\xi W(w)\rho = 0. \tag{54}$$

The four eigenvalues ρ_i $(i = 1, 2, 3, 4)$ at each equilibrium state $(0, 0, 0, w)$ can be written as

$$\left.\begin{aligned} &\rho_{1,2} \approx -0.189912 \pm i\ 4.37021, \quad \rho_3 \approx 8.77982, \quad \rho_4 = 0, \quad \text{for } |w| < 1, \\ &\rho_{1,2} \approx 0.0546351 \pm i\ 4.46535, \quad \rho_3 \approx -37.9093, \quad \rho_4 = 0, \quad \text{for } |w| > 1. \end{aligned}\right\} \tag{55}$$

Thus, they are characterized by an unstable saddle-focus except for the zero eigenvalue.

3.2. *A third-order canonical memristor oscillator*

Removing a capacitor (resp. an inductor) from the circuit of Fig. 7 (resp. Fig. 8), we obtain the third-order oscillator in Fig. 14 (resp. Fig. 15). Applying Kirchhoff's circuit laws to node A and loop C of the circuit in Fig. 16, we obtain

$$\left.\begin{aligned} i_1 &= i_3 - i, \\ v_3 &= v_4 - v_1. \end{aligned}\right\} \tag{56}$$

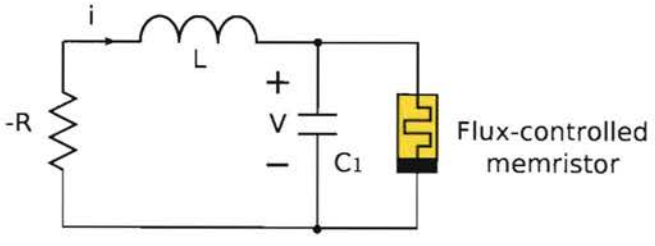

Fig. 14. A third-order oscillator with a flux-controlled memristor.

Integrating Eq. (56) with respect to time t, we obtain a set of equations which define the relation between the charge and the flux:

$$\left.\begin{aligned} q_1 &= q_3 - q(\varphi), \\ \varphi_3 &= \varphi_4 - \varphi_1, \end{aligned}\right\} \tag{57}$$

where

$$\left.\begin{aligned} q_1 &\triangleq \int_{-\infty}^{t} i_1(t)dt, \\ q_3 &\triangleq \int_{-\infty}^{t} i_3(t)dt, \\ q &\triangleq \int_{-\infty}^{t} i(t)dt, \end{aligned}\right\} \quad \left.\begin{aligned} \varphi_1 &\triangleq \int_{-\infty}^{t} v_1(t)dt, \\ \varphi_3 &\triangleq \int_{-\infty}^{t} v_3(t)dt, \\ \varphi_4 &\triangleq \int_{-\infty}^{t} v_4(t)dt, \\ \varphi &\triangleq \int_{-\infty}^{t} v(t)dt = \varphi_1. \end{aligned}\right\} \tag{58}$$

Here, the symbols q_1, q_3, and q denote the *charge* of capacitor C_1, inductor L, and the memristor, respectively, and the symbols $\varphi_1, \varphi_3, \varphi_4$ and φ denote the *flux* of capacitor C_1, inductor L,

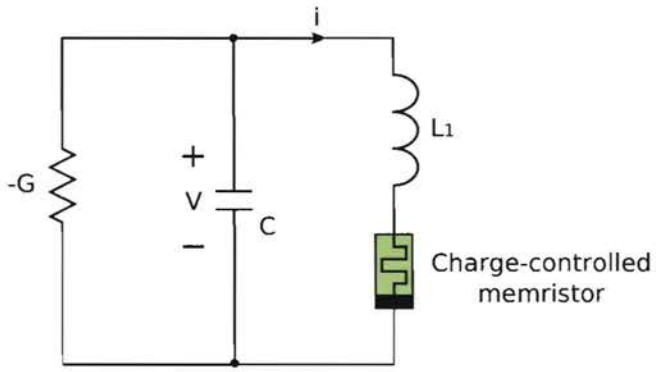

Fig. 15. Dual circuit with a charge-controlled memristor.

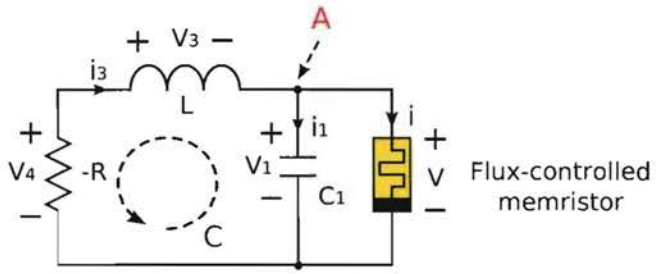

Fig. 16. Currents i_j, voltages v_j, node A, and loop C are indicated.

resistance $-R$, and the memristor, respectively.[8] The $\varphi - q$ characteristic curve of the memristor is given by

$$q(\varphi) = b\varphi + 0.5(a-b)(|\varphi+1| - |\varphi-1|). \quad (59)$$

Solving Eq. (57) for (q_3, φ_4), we get

$$\left.\begin{aligned} q_3 &= q_1 + q(\varphi), \\ \varphi_4 &= \varphi + \varphi_3. \end{aligned}\right\} \quad (60)$$

Thus, $(q_1, \varphi, \varphi_3)$ can be chosen to be the independent variables, namely, the charge of capacitor C_1, the flux of inductor L, and the flux of the memristor, respectively.

From Eq. (56) (or differentiating Eq. (57) with respect to time t), we obtain a set of three first-order differential equations, which defines the relation among the three variables (v_1, i_3, φ):

$$\left.\begin{aligned} C_1\frac{dv_1}{dt} &= i_3 - W(\varphi)v_1, \\ L\frac{di_3}{dt} &= Ri_3 - v_1, \\ \frac{d\varphi}{dt} &= v_1, \end{aligned}\right\} \quad (61)$$

where

$$\left.\begin{aligned} \frac{dq_1}{dt} &= i_1 = C_1\frac{dv_1}{dt}, \\ \frac{dq_3}{dt} &= i_3, \\ \frac{d\varphi_1}{dt} &= v_1, \end{aligned}\right\} \quad \left.\begin{aligned} \frac{d\varphi_3}{dt} &= v_3 = L\frac{di_3}{dt}, \\ \frac{d\varphi_4}{dt} &= v_4 = Ri_3, \\ W(\varphi) &= \frac{dq(\varphi)}{d\varphi}. \end{aligned}\right\} \quad (62)$$

Note that the two kinds of independent variables are related by

$$\boxed{\begin{array}{c} (q_1, \varphi, \varphi_3) \longleftrightarrow (v_1, \varphi, i_3) \\ q_1 = C_1 v_1, \ \varphi_3 = Li_3 \end{array}} \quad (63)$$

Thus, Eq. (61) can be recast into the following set of differential equations using only charge and flux as variables:

$$\left.\begin{aligned} \frac{dq_1}{dt} &= \frac{\varphi_3}{L} - \frac{W(\varphi)q_1}{C_1}, \\ \frac{d\varphi_3}{dt} &= \frac{R\varphi_3}{L} - \frac{q_1}{C_1}, \\ \frac{d\varphi}{dt} &= \frac{q_1}{C_1}. \end{aligned}\right\} \quad (64)$$

We next study the behavior of this circuit. Equation (61) can be transformed into the form

$$\left.\begin{aligned} \frac{dx}{dt} &= \alpha(y - W(z)x), \\ \frac{dy}{dt} &= -\xi x + \beta y, \\ \frac{dz}{dt} &= x, \end{aligned}\right\} \quad (65)$$

where $x = v_1$, $y = i_3$, $z = \varphi$, $\alpha = 1/C_1$, $\xi = 1/L$, $\beta = R/L$, and the piecewise-linear functions $q(z)$ and $W(z)$ are given by

$$\left.\begin{aligned} q(z) &= bz + 0.5(a-b)(|z+1| - |z-1|), \\ W(z) &= \frac{dq(z)}{dz} = \begin{cases} a, & |z| < 1, \\ b, & |z| > 1, \end{cases} \end{aligned}\right\} \quad (66)$$

respectively, where $a, b > 0$.

The equilibrium state of Eq. (65) is given by the set $A \triangleq \{(x, y, z) | x = y = 0, \ z = \text{constant}\}$, which corresponds to the z-axis. The Jacobian matrix D

[8]The term "*charge*" and "*flux*" are just *names* given to the definition in Eq. (58), and should not be interpreted as a *physical* charge or flux in the classical sense. The important concept here is that they are *measurable* quantities, obtained via integration.

at this equilibrium set is given by

$$D = \begin{bmatrix} -\alpha W(z) & \alpha & 0 \\ -\xi & \beta & 0 \\ 1 & 0 & 0 \end{bmatrix}, \tag{67}$$

and its characteristic equation is given by

$$\rho^3 + (\alpha W(z) - \beta)\rho^2 + \alpha(\xi - \beta W(z))\rho = 0. \tag{68}$$

If we set $\alpha = 1$, $\beta = 0.1$, $\xi = 1$, $a = 0.02$, and $b = 2$, then it has three eigenvalues λ_i $(i = 1, 2, 3)$:

$$\left.\begin{array}{lll} \lambda_{1,2} \approx 0.04 \pm i\ 0.998198, \quad \lambda_3 \approx 0, & & \text{for } |z| < 1, \\ \lambda_1 \approx -1.27016, \quad \lambda_2 \approx -0.629844, \quad \lambda_3 = 0, & & \text{for } |z| > 1. \end{array}\right\} \tag{69}$$

Thus, the set $B \triangleq \{(x, y, z) | x = y = 0, |z| < 1\}$ is unstable, and the set $C \triangleq \{(x, y, z) | x = y = 0, |z| > 1\}$ is stable. Our computer simulation shows that Eq. (65) has two distinct stable periodic attractors as shown in Fig. 17. Observe that they are odd symmetric images of each other, as expected in view of the odd-symmetric characteristic $q = q(\varphi)$ of the memristor in Eq. (66).

Equation (65) can be transformed into the form

$$\frac{d^2y}{dt^2} + (\alpha W(z) - \beta)\frac{dy}{dt} + \alpha(\xi - \beta W(z))y = 0, \tag{70}$$

or equivalently

$$\left.\begin{array}{ll} \dfrac{d^2y}{dt^2} + (a\alpha - \beta)\dfrac{dy}{dt} + \alpha(\xi - a\beta)y = 0, & \text{for } |z| < 1, \\ \dfrac{d^2y}{dt^2} + (b\alpha - \beta)\dfrac{dy}{dt} + \alpha(\xi - b\beta)y = 0, & \text{for } |z| > 1. \end{array}\right\} \tag{71}$$

Thus, Eq. (65) can be interpreted as a second-order linear differential equation over the domain of the state variable z whose dynamics evolves according to $dz/dt = x$ in Eq. (65). Furthermore, if we substitute

$$\left.\begin{array}{l} u(t) \triangleq \displaystyle\int_0^t y(t)dt + c, \\ z(t) = \xi^{-1}\left\{\beta u(t) - \dfrac{du(t)}{dt}\right\} + d, \end{array}\right\} \tag{72}$$

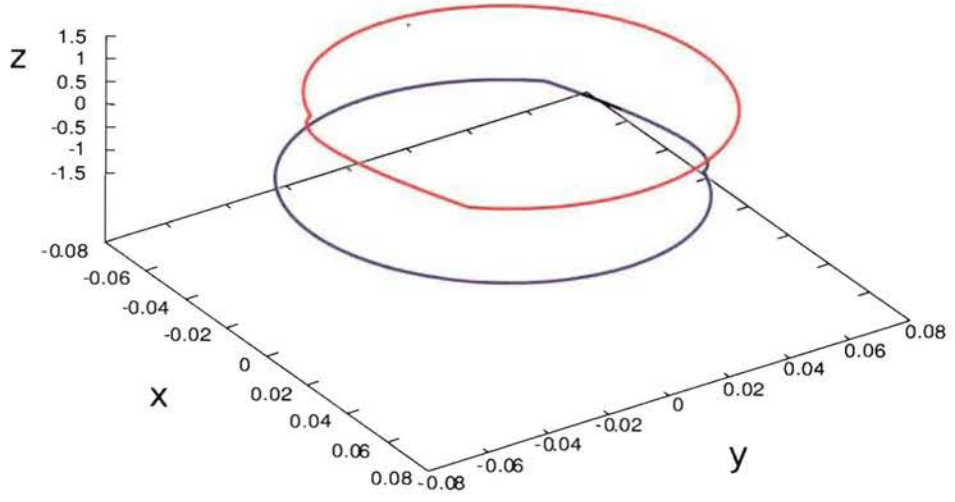

Fig. 17. Two periodic attractors of the third-order canonical memristor oscillator.

into Eq. (70) (c and d are constants), we would obtain the following third-order differential equation

$$\frac{d^3u}{dt^3}+\left[\alpha W\left(\xi^{-1}\left\{\beta u(t)-\frac{du(t)}{dt}\right\}+d\right)-\beta\right]\frac{d^2u}{dt^2}+\alpha\left[\xi-\beta W\left(\xi^{-1}\left\{\beta u(t)-\frac{du(t)}{dt}\right\}+d\right)\right]\frac{du}{dt}=0, \tag{73}$$

in terms of u, or equivalently

$$\left.\begin{aligned}&\frac{d^3u}{dt^3}+(a\alpha-\beta)\frac{d^2u}{dt^2}+\alpha(\xi-a\beta)\frac{du}{dt}=0, \quad \text{for}\left|\xi^{-1}\left\{\beta u(t)-\frac{du(t)}{dt}\right\}+d\right|<1,\\ &\frac{d^3u}{dt^3}+(b\alpha-\beta)\frac{d^2u}{dt^2}+\alpha(\xi-b\beta)\frac{du}{dt}=0, \quad \text{for}\left|\xi^{-1}\left\{\beta u(t)-\frac{du(t)}{dt}\right\}+d\right|>1.\end{aligned}\right\} \tag{74}$$

They can be written as

$$\frac{d}{dt}\left[\frac{d^2u}{dt^2}+\left[\alpha W\left(\xi^{-1}\left\{\beta u(t)-\frac{du(t)}{dt}\right\}+d\right)-\beta\right]\frac{du}{dt}+\alpha\left[\xi-\beta W\left(\xi^{-1}\left\{\beta u(t)-\frac{du(t)}{dt}\right\}+d\right)\right]u\right]=0, \tag{75}$$

and

$$\left.\begin{aligned}&\frac{d}{dt}\left\{\frac{d^2u}{dt^2}+(a\alpha-\beta)\frac{du}{dt}+\alpha(\xi-a\beta)u\right\}=0, \quad \text{for}\left|\xi^{-1}\left\{\beta u(t)-\frac{du(t)}{dt}\right\}+d\right|<1,\\ &\frac{d}{dt}\left\{\frac{d^2u}{dt^2}+(b\alpha-\beta)\frac{du}{dt}+\alpha(\xi-b\beta)u\right\}=0, \quad \text{for}\left|\xi^{-1}\left\{\beta u(t)-\frac{du(t)}{dt}\right\}+d\right|>1,\end{aligned}\right\} \tag{76}$$

respectively. Note that $dW(z)/dz = 0$. Since the characteristic equation of Eqs. (73) and (74) have a zero-eigenvalue everywhere, and Eq. (76) can be interpreted as a second-order linear differential equation, Eq. (65) does not have a chaotic attractor, even if the circuit elements are active.

Consider next the three-element circuit in Fig. 18, obtained by short circuiting the resistor from Fig. 14 (its dual circuit is shown in Fig. 19). The dynamics of this circuit can be written as

$$\left.\begin{aligned}\frac{dx}{dt}&=\alpha\big(y-W(z)x\big),\\ \frac{dy}{dt}&=-\xi x,\\ \frac{dz}{dt}&=x.\end{aligned}\right\} \tag{77}$$

From this equation, we obtain

$$\frac{d}{dt}\left\{\frac{1}{2}\left(\frac{x^2}{\alpha}+\frac{y^2}{\xi}\right)\right\}=-W(z)x^2\le 0. \tag{78}$$

Hence, the z-axis is globally asymptotically stable. From Eq. (77), we obtain

$$\frac{dy}{dt}+\xi\frac{dz}{dt}=0. \tag{79}$$

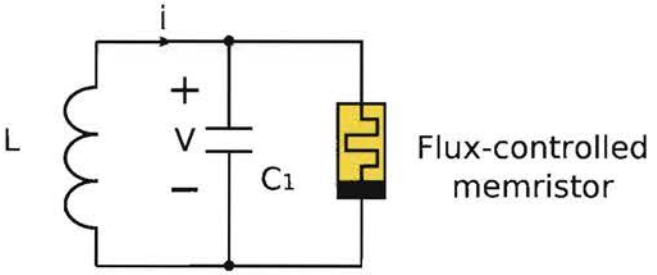

Fig. 18. A third-order circuit with a flux-controlled memristor.

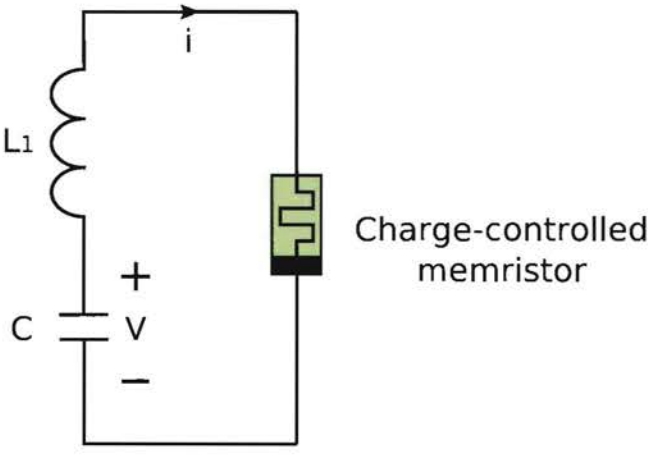

Fig. 19. Dual circuit with a charge-controlled memristor.

Thus, $y(t)$ and $z(t)$ satisfy

$$z(t) = \frac{-y(t) + y_0}{\xi}, \tag{80}$$

where y_0 is a constant. Since $W(z) = W(y_0 - y)$, Eq. (77) can be transformed into the form

$$\frac{d^2y}{dt^2} + \alpha W\left(\frac{y_0 - y}{\xi}\right)\frac{dy}{dt} + \alpha y = 0. \tag{81}$$

Thus, Eq. (77) is equivalent to a one-parameter family of second-order differential equations. Since the minimal dimension for a continuous chaotic system is 3, Eq. (77) cannot have a chaotic attractor, even if the circuit elements are active. We will discuss this observation in Sec. 4.2.

3.3. *A second-order canonical memristor circuit*

If we remove an inductor (resp. a capacitor) from Fig. 14 (resp. Fig. 15), we would obtain the second-order circuit in Fig. 20 (resp. Fig. 21). Applying the Kirchhoff's circuit laws to the circuit in Fig. 22, we obtain

$$i_1 = i_3 - i. \tag{82}$$

Integrating Eq. (82) with respect to time t, we obtain a set of equations which define a relation between the charge and the flux:

$$q_1 = q_3 - q(\varphi), \tag{83}$$

where

$$\left.\begin{aligned} q_1 &\triangleq \int_{-\infty}^{t} i_1(t)dt, \\ q_3 &\triangleq \int_{-\infty}^{t} i_3(t)dt, \\ q &\triangleq \int_{-\infty}^{t} i(t)dt, \\ \varphi &\triangleq \int_{-\infty}^{t} v(t)dt. \end{aligned}\right\} \tag{84}$$

Here, the symbols q_1, q_3, and q denote the charge of capacitor C_1, conductance $-G$, and the memristor, and the symbol φ denotes the flux of memristor,

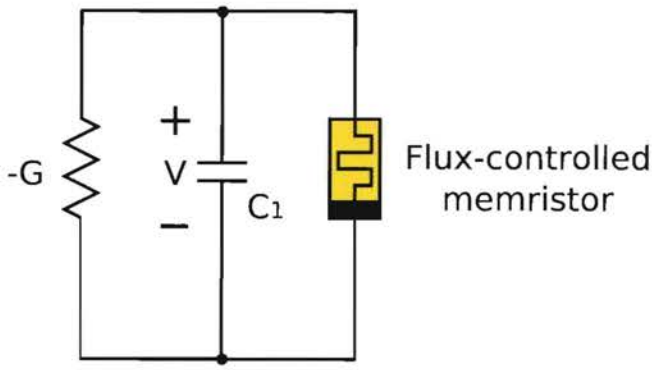

Fig. 20. A second-order circuit with a flux-controlled memristor.

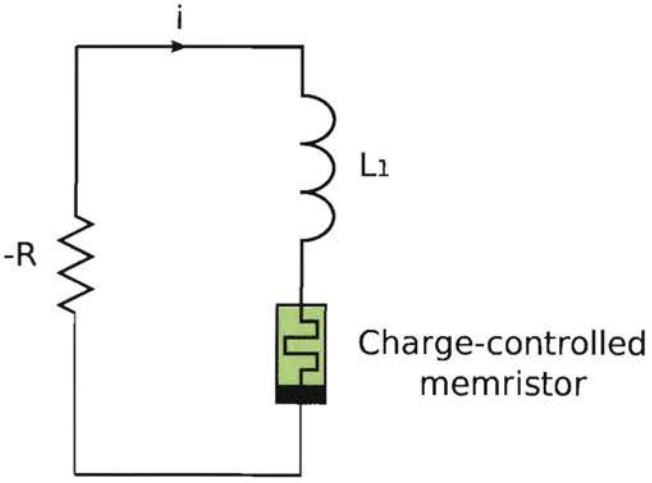

Fig. 21. Dual circuit with a charge-controlled memristor.

respectively. The $\varphi - q$ characteristic curve of the memristor is given by

$$q(\varphi) = b\varphi + 0.5(a - b)(|\varphi + 1| - |\varphi - 1|). \tag{85}$$

Solving Eq. (83) for q_3, we obtain

$$q_3 = q_1 + q(\varphi). \tag{86}$$

Thus, q_1 and φ can be chosen as independent variables.

From Eq. (82) (or differentiating Eq. (83) with respect to time t), we obtain a set of two first-order differential equations:

$$\left.\begin{aligned} C_1\frac{dv_1}{dt} &= (G - W(\varphi))v_1, \\ \frac{d\varphi}{dt} &= v_1, \end{aligned}\right\} \tag{87}$$

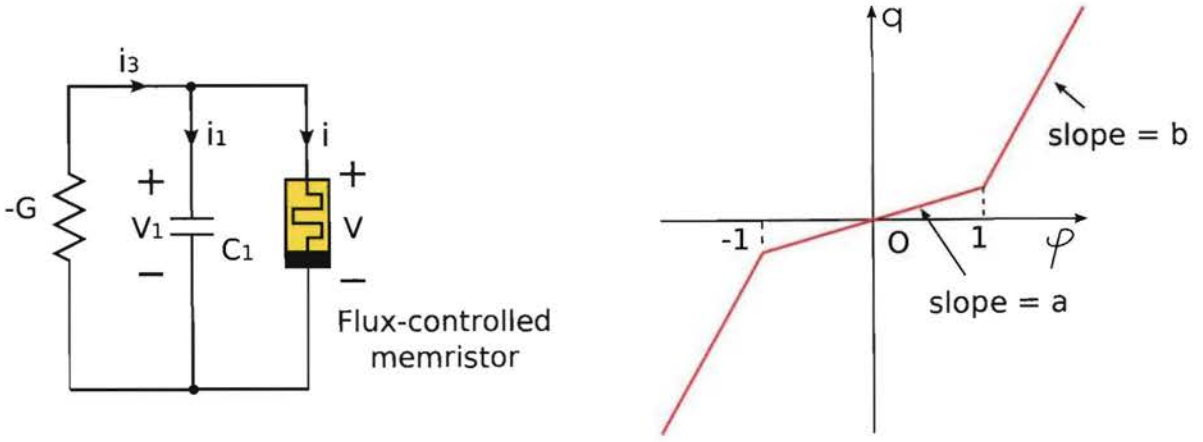

Fig. 22. The circuit from Fig. 20 and the $\varphi - q$ characteristic of the flux-controlled memristor defined by Eq. (85). Currents i_1, i_3 and voltage v_1 are indicated.

where

$$\left.\begin{aligned} \frac{dq_1}{dt} &= i_1 = C_1 \frac{dv_1}{dt}, \\ \frac{dq_3}{dt} &= i_3 = G v_1, \\ W(\varphi) &= \frac{dq(\varphi)}{d\varphi}. \end{aligned}\right\} \tag{88}$$

Note that the two kinds of independent variables are related by

$$\boxed{\begin{array}{c} (q_1, \varphi) \longleftrightarrow (v_1, \varphi) \\ q_1 = C_1 v_1 \end{array}} \tag{89}$$

Thus, Eq. (87) can be recast in terms of the charge and the flux as state variables:

$$\left.\begin{aligned} \frac{dq_1}{dt} &= (G - W(\varphi)) \frac{q_1}{C_1}, \\ \frac{d\varphi}{dt} &= \frac{q_1}{C_1}. \end{aligned}\right\} \tag{90}$$

We next study the behavior of this circuit. Equation (87) can be transformed into the form

$$\left.\begin{aligned} \frac{dx}{dt} &= \alpha(\beta - W(y))x, \\ \frac{dy}{dt} &= x, \end{aligned}\right\} \tag{91}$$

where $x = v_1$, $y = \varphi$, $\alpha = 1/C$, $\beta = G$, and the piecewise-linear functions $q(y)$ and $W(y)$ are given by

$$\left.\begin{aligned} q(y) &= by + 0.5(a-b)(|y+1| - |y-1|), \\ W(y) &= \frac{dq(y)}{dy} = \begin{cases} a, & |y| < 1, \\ b, & |y| > 1, \end{cases} \end{aligned}\right\} \tag{92}$$

respectively, where $a, b > 0$. The first equation of Eq. (91) can be written as

$$\frac{dx}{dt} = \begin{cases} \alpha(\beta - a)x, & |y| < 1, \\ \alpha(\beta - b)x, & |y| > 1. \end{cases} \tag{93}$$

Thus, the solution of Eq. (93) for $|y| < 1$ and $|y| > 1$ can be expressed as

$$x(t) = x_0 e^{\alpha(\beta - a)t}, \tag{94}$$

and

$$x(t) = x_0 e^{\alpha(\beta - b)t}, \tag{95}$$

respectively, where $x(0) = x_0$ is the initial condition for $t = 0$. If we set $a = 0.01$, $b = 0.05$. $\alpha = 1$, $\beta = 0.03$ and $e = 10$, our computer simulation shows that $x(t) \to 0$ for $t \to \infty$ as shown in Fig. 23. Thus, this second-order circuit does not oscillate.

4. Memristor-Based Chua Oscillators

In this section, we design a nonlinear oscillator by replacing "*Chua's diode*" with an active two-terminal circuit consisting of a negative conductance and a memristor (or an active memristor). We derive a set of differential equations from the nonlinear circuit directly.

4.1. *A fourth-order memristor-based Chua oscillator*

Consider Chua's oscillator in Fig. 24. If we replace Chua's diode with an active two-terminal circuit

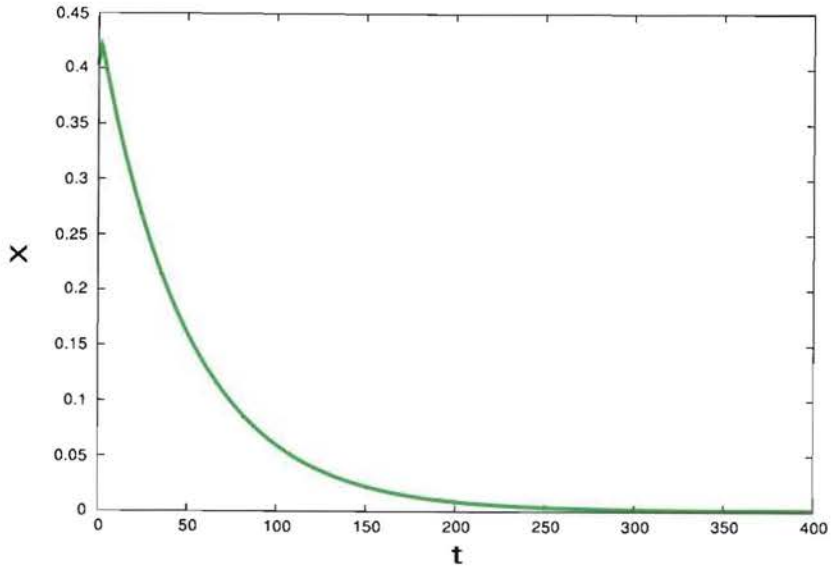

Fig. 23. Solution of the second-order circuit in Fig. 22.

consisting of a conductance and a flux-controlled memristor, we would obtain the circuit as in Fig. 25. The dynamics of the circuit in Fig. 25 is given by the following set of four first-order differential equations

$$\left.\begin{aligned} C_1\frac{dv_1}{dt} &= \frac{v_2 - v_1}{R} + Gv_1 - W(\varphi)v_1, \\ C_2\frac{dv_2}{dt} &= \frac{v_1 - v_2}{R} - i, \\ L\frac{di}{dt} &= v_2 - ri, \\ \frac{d\varphi}{dt} &= v_1, \end{aligned}\right\} \tag{96}$$

where

$$\left.\begin{aligned} q(\varphi) &= b\varphi + 0.5(a-b)(|\varphi+1| - |\varphi-1|), \\ W(\varphi) &= \frac{dq(\varphi)}{d\varphi}. \end{aligned}\right\} \tag{97}$$

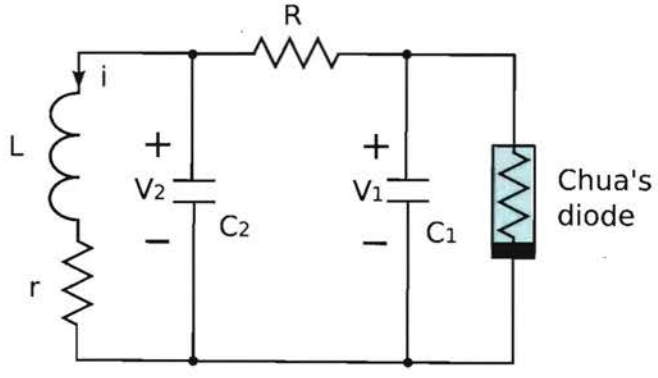

Fig. 24. Chua's oscillator.

Equation (96) can be transformed into the form

$$\left.\begin{aligned} \frac{dx}{dt} &= \alpha(y - x + \xi x - W(w)x), \\ \frac{dy}{dt} &= x - y + z, \\ \frac{dz}{dt} &= -\beta y - \gamma z, \\ \frac{dw}{dt} &= x, \end{aligned}\right\} \tag{98}$$

where we set

$$\left.\begin{aligned} x &= v_1, \quad y = v_2, \quad z = -i, \quad w = \varphi, \\ \alpha &= \frac{1}{C_1}, \quad \beta = \frac{1}{L}, \quad \gamma = \frac{r}{L}, \quad \xi = G, \\ C_2 &= 1, \quad R = 1, \end{aligned}\right\} \tag{99}$$

and the piecewise-linear functions $q(w)$ and $W(w)$ are given by

$$\left.\begin{aligned} q(w) &= bw + 0.5(a-b)(|w+1| - |w-1|), \\ W(w) &= \begin{cases} a, & |w| < 1, \\ b, & |w| > 1, \end{cases} \end{aligned}\right\} \tag{100}$$

respectively, where $a, b > 0$. If we set $\alpha = 10$, $\beta = 13$, $\gamma = 0.35$, $\xi = 1.5$, $a = 0.3$ and $b = 0.8$, our computer simulation shows that Eq. (98) has a chaotic attractor as shown in Fig. 26. By calculating the Lyapunov exponents from sampled time series, we found that this chaotic attractor has one positive Lyapunov exponent $\lambda_1 = 0.0779$.

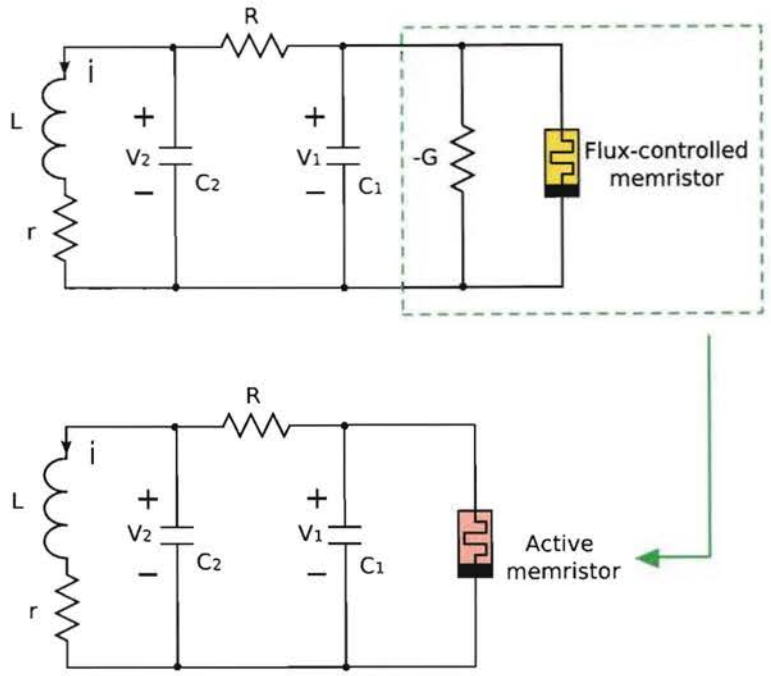

Fig. 25. Chua's oscillator with a flux-controlled memristor and a negative conductance.

The equilibrium state of Eq. (98) is given by $A = \{(x, y, z, w) | x = y = z = 0,\ w = \text{constant}\}$, which corresponds to the w-axis. The Jacobian matrix D at this equilibrium set is given by

$$D = \begin{bmatrix} \alpha(-1 + \xi - W(w)) & \alpha & 0 & 0 \\ 1 & -1 & 1 & 0 \\ 0 & -\beta & -\gamma & 0 \\ 1 & 0 & 0 & 0 \end{bmatrix}, \tag{101}$$

and its four eigenvalues ρ_i $(i = 1, 2, 3, 4)$ can be written as

$$\left.\begin{array}{llll} \rho_{1,2} \approx -1.31104 \pm i\ 2.74058, & \rho_3 \approx 3.27207, & \lambda_4 = 0, & \text{for } |w| < 1, \\ \rho_{1,2} \approx 0.0786554 \pm i\ 2.84655, & \rho_3 \approx -4.50731, & \rho_4 = 0, & \text{for } |w| > 1. \end{array}\right\} \tag{102}$$

Thus, they are characterized by an unstable saddle-focus except for the zero eigenvalue.

4.2. *A third-order memristor-based Chua oscillator*

Consider next the Van der Pol oscillator with Chua's diode as illustrated in Fig. 27. If we replace Chua's diode with a two-terminal circuit consisting of a conductance and a flux-controlled memristor, we would obtain the circuit shown in Fig. 28. The dynamics of this circuit is given by

$$\left.\begin{aligned} C\frac{dv}{dt} &= -i - W(\varphi)v + Gv, \\ L\frac{di}{dt} &= v, \\ \frac{d\varphi}{dt} &= v, \end{aligned}\right\} \tag{103}$$

where

$$\left.\begin{aligned} W(\varphi) &= \frac{dq(\varphi)}{d\varphi}, \\ q(\varphi) &= b\varphi + 0.5(a - b)(|\varphi + 1| - |\varphi - 1|). \end{aligned}\right\} \tag{104}$$

Equation (103) can be transformed into the form

$$\left.\begin{aligned} \frac{dx}{dt} &= \alpha(-y - W(z)x + \gamma x), \\ \frac{dy}{dt} &= \beta x, \\ \frac{dz}{dt} &= x, \end{aligned}\right\} \tag{105}$$

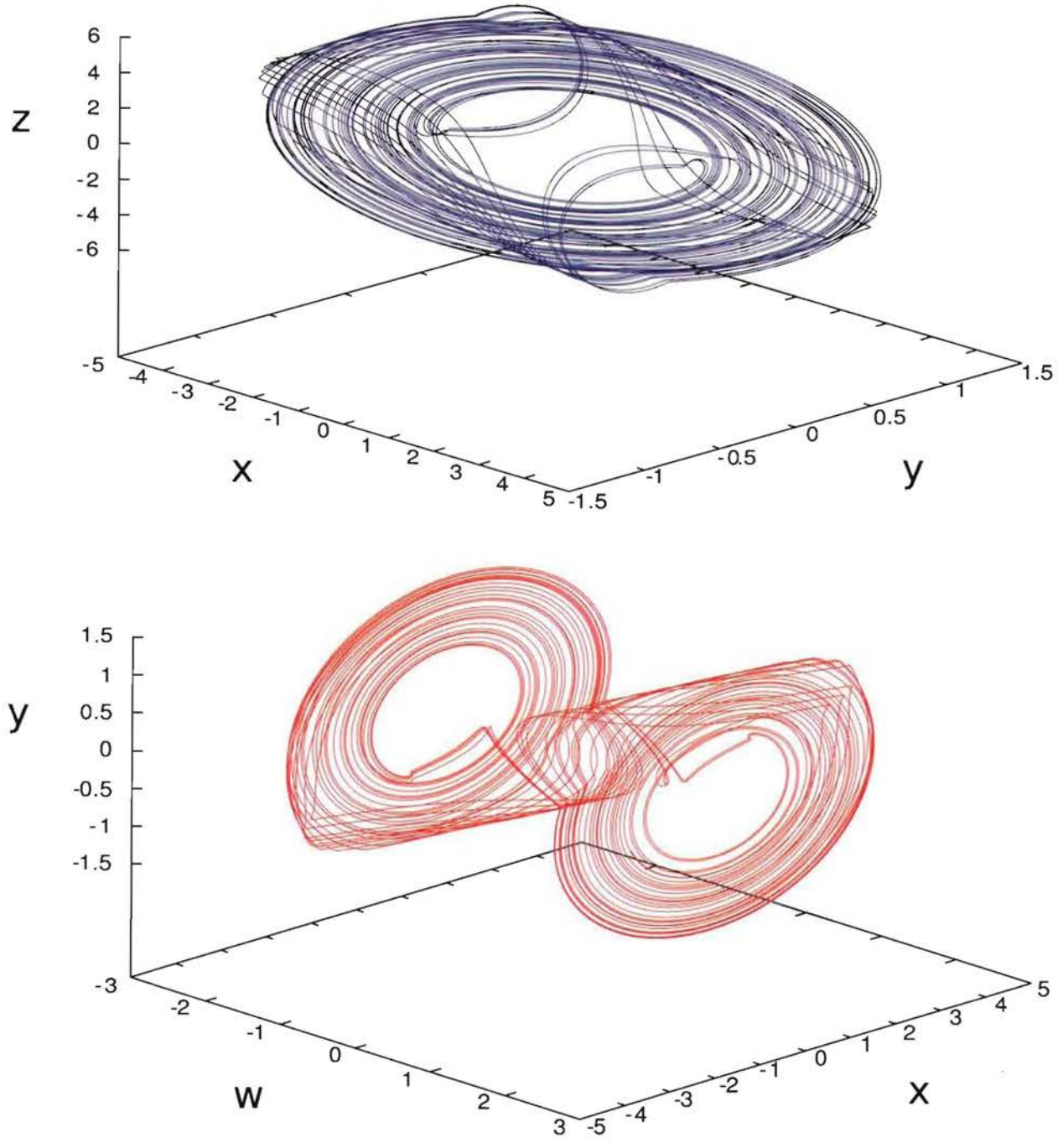

Fig. 26. Chaotic attractor of Chua's oscillator with a flux-controlled memristor and a negative conductance.

where $x = v,\ y = i,\ z = \varphi,\ \alpha = 1/C,\ \beta = 1/L,$ $\gamma = G$, and the piecewise-linear functions $q(z)$ and $W(z)$ are given by

$$\left.\begin{aligned} q(z) &= bz + 0.5(a-b)(|z+1| - |z-1|), \\ W(z) &= \begin{cases} a, & |z| < 1, \\ b, & |z| > 1, \end{cases} \end{aligned}\right\} \quad (106)$$

respectively, where $a, b > 0$. From Eq. (105), we obtain

$$\frac{dy}{dt} - \beta\frac{dz}{dt} = 0. \quad (107)$$

Thus, $y(t)$ and $z(t)$ satisfy

$$z(t) = \frac{y(t) + c}{\beta}, \quad (108)$$

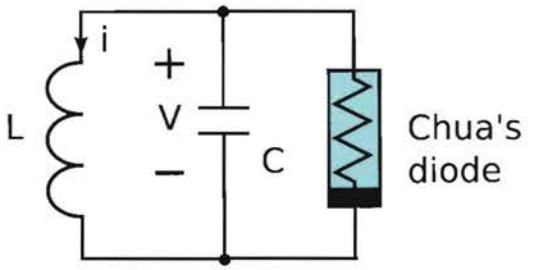

Fig. 27. Van der Pol oscillator.

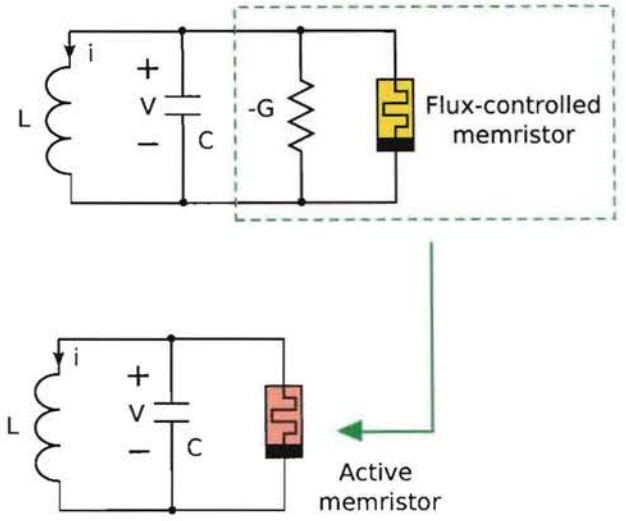

Fig. 28. A third-order oscillator with a flux-controlled memristor and a negative conductance.

where c is constant. Since $W(z) = W((y+c)/\beta)$, Eq. (105) can be transformed into the form

$$\frac{d^2y}{dt^2} + \alpha\left\{W\left(\frac{y+c}{\beta}\right) - \gamma\right\}\frac{dy}{dt} + \alpha\beta y = 0, \quad (109)$$

or equivalently

$$\left.\begin{aligned} \frac{d^2y}{dt^2} + \alpha(a-\gamma)\frac{dy}{dt} + \alpha\beta y = 0, \quad |z| < 1, \\ \frac{d^2y}{dt^2} + \alpha(b-\gamma)\frac{dy}{dt} + \alpha\beta y = 0, \quad |z| > 1. \end{aligned}\right\} \quad (110)$$

Thus, Eq. (105) is equivalent to a one-parameter family of second-order differential equations, parametrized by the constant "c", via Eq. (108). Since the minimal dimension for a continuous chaotic system is 3, Eq. (105) cannot have a chaotic attractor, even if the circuit elements are active. If we set $\alpha = 2, \gamma = 0.3, \beta = 1, a = 0.1$ and $b = 0.5$, our computer simulation shows that Eq. (105) has two periodic attractors as shown in Fig. 29. Observe that these two limit cycles are odd-symmetric images of each other, as expected. The equilibrium state of Eq. (105) is given by $A = \{(x, y, z) | x = y = 0, z = \text{constant}\}$, which corresponds to the z-axis. The Jacobian matrix D at this equilibrium set is given by

$$D = \begin{bmatrix} \alpha(\gamma - W(z)) & -\alpha & 0 \\ \beta & 0 & 0 \\ 1 & 0 & 0 \end{bmatrix}. \quad (111)$$

Its characteristic equation and eigenvalues λ_i $(i = 1, 2, 3)$ can be written as

$$\left.\begin{aligned} \rho(\rho^2 + \alpha(a-\gamma)\rho + \alpha\beta) = 0, \quad |z| < 1, \\ \rho(\rho^2 + \alpha(b-\gamma)\rho + \alpha\beta) = 0, \quad |z| > 1, \end{aligned}\right\} \quad (112)$$

and

$$\left.\begin{aligned} \lambda_{1,2} = 0.2 \pm i\ 1.4, \quad \lambda_3 = 0, \quad \text{for } |z| < 1, \\ \lambda_{1,2} = -0.2 \pm i\ 1.4, \quad \lambda_3 = 0, \quad \text{for } |z| > 1, \end{aligned}\right\} \quad (113)$$

respectively. Thus, the equilibrium set is unstable if $|z| < 1$, and stable if $|z| > 1$.

4.3. *A second-order memristor-based circuit*

Consider again the Van der Pol oscillator with the voltage-controlled Chua's diode from [Barboza & Chua, 2008], as illustrated in Fig. 27. If we let the capacitance $C \to 0$, we would obtain the relaxation oscillator shown in Fig. 30, which exhibits a jump behavior [Chua, 1969]. Furthermore, by replacing Chua's diode in Fig. 30 with a two-terminal circuit consisting of a conductance and a flux-controlled memristor, we obtain the circuit of Fig. 31. The dynamics of the circuit in Fig. 31 is given by

$$\left.\begin{aligned} i &= (G - W(\varphi))v, \\ L\frac{di}{dt} &= v, \\ \frac{d\varphi}{dt} &= v, \end{aligned}\right\} \quad (114)$$

where

$$\left.\begin{aligned} W(\varphi) &= \frac{dq(\varphi)}{d\varphi}, \\ q(\varphi) &= b\varphi + 0.5(a-b) \\ &\quad \times (|\varphi + 1| - |\varphi - 1|). \end{aligned}\right\} \quad (115)$$

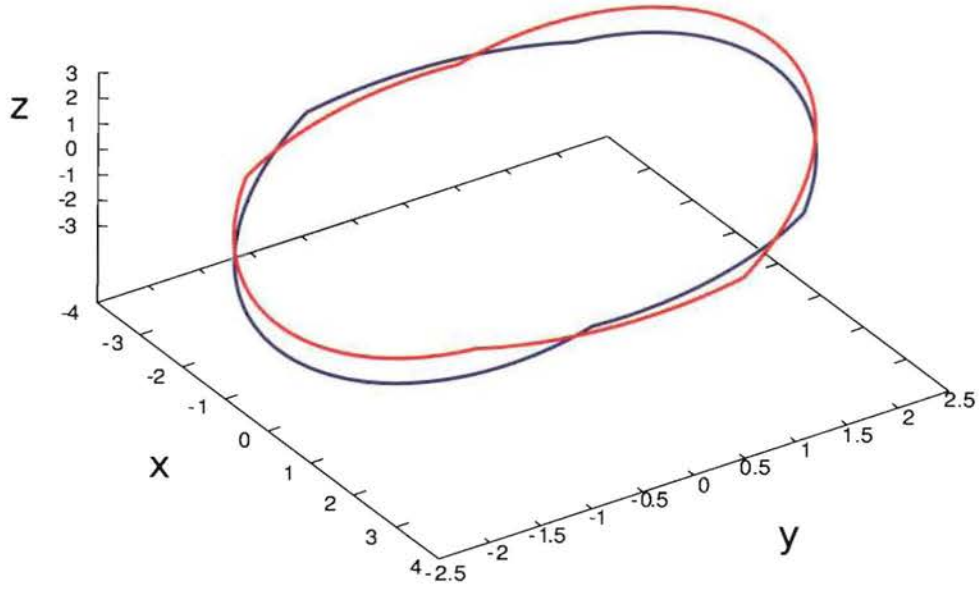

Fig. 29. Two periodic attractors of the third-order memristor oscillator.

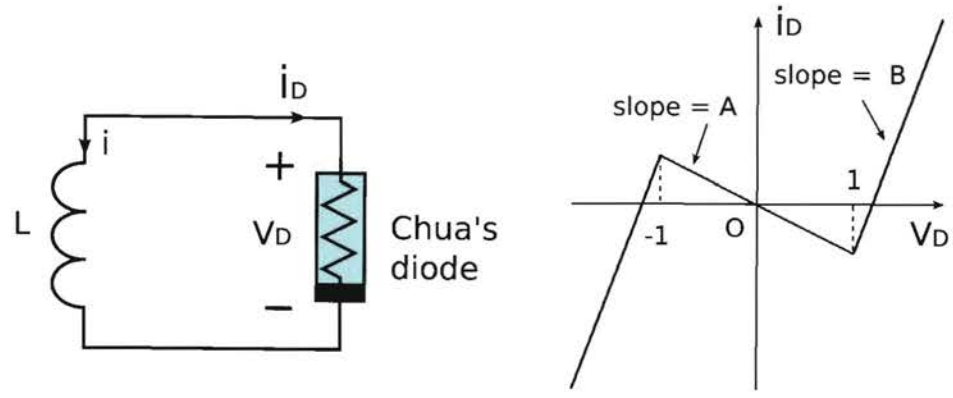

Fig. 30. A relaxation oscillator where the $v_D - i_D$ curve of Chua's diode is given by Fig. 15 of [Barboza & Chua, 2008].

Equation (114) can be written as

$$\left.\begin{aligned} y &= (\gamma - W(z))x, \\ \frac{dy}{dt} &= \beta x, \\ \frac{dz}{dt} &= x, \end{aligned}\right\} \tag{116}$$

where $x = v, y = i, z = \varphi, \beta = 1/L, G = \gamma$. From Eq. (116), we obtain

$$\frac{dy}{dt} - \beta\frac{dz}{dt} = 0. \tag{117}$$

Thus, $y(t)$ and $z(t)$ satisfy

$$y(t) - \beta z(t) = c, \tag{118}$$

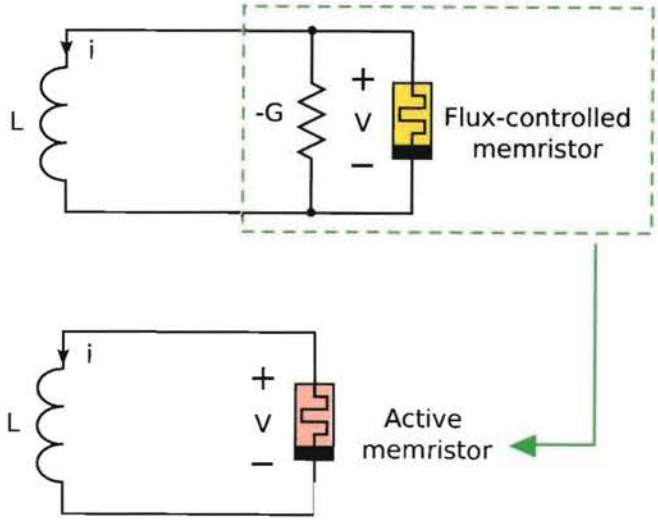

Fig. 31. A second-order oscillator.

where c is a constant. From Eq. (116), we obtain

$$y = (\gamma - W(z))x = (\gamma - W(z))\frac{dz}{dt}. \tag{119}$$

We can interpret Eq. (119) as a one-parameter family of first-order differential equations, namely,

$$\begin{aligned}\frac{dz}{dt} &= \frac{y}{\gamma - W(z)} \\ &= \frac{\beta z + c}{\gamma - W(z)} \\ &= \begin{cases} \dfrac{\beta z + c}{\gamma - a}, & |z| < 1, \\ \dfrac{\beta z + c}{\gamma - b}, & |z| > 1. \end{cases}\end{aligned} \tag{120}$$

The solution of Eq. (120) for $|z| < 1$ and $|z| > 1$ can be expressed as

$$z(t) = de^{\frac{\beta}{\gamma - a}t} - \frac{c}{\beta}, \tag{121}$$

and

$$z(t) = de^{\frac{\beta}{\gamma - b}t} - \frac{c}{\beta}, \tag{122}$$

respectively, where c and d are constants.

If we replace the piecewise-linear function of the memristor by a smooth cubic function, namely

$$\left.\begin{aligned} q(z) &= \frac{z^3}{3}, \\ W(z) &= z^2, \end{aligned}\right\} \tag{123}$$

we would obtain

$$\frac{dz}{dt} = \frac{\beta z + c}{\gamma - z^2}. \tag{124}$$

If we set $\gamma = 1, \beta = 1$ and $c = 1$, the correct solution of Eq. (124) is given by

$$z(t) = 1 \pm \sqrt{2\,(e - t)}, \tag{125}$$

where e is a constant, and shown in Fig. 32. Our computer simulation shows that Eq. (124) exhibits the *incorrect* irregular oscillation shown in Fig. 33. This erroneous computer-generated solution is caused by the numerical integration error at $z = \pm 1$.

4.4. *First-order memristor-based circuit*

Consider the circuit in Fig. 34, which consists of a current source J and a two-terminal circuit consisting of a conductance and a flux-controlled memristor. The circuit equation of Fig. 34 can be written as

$$\int (J + Gv)dt = q(\varphi), \tag{126}$$

where $q(\varphi)$ denotes the characteristic of the memristor. Differentiating Eq. (126) with respect to time t, we obtain

$$\left.\begin{aligned} J + Gv &= W(\varphi)v, \\ \frac{d\varphi}{dt} &= v, \end{aligned}\right\} \tag{127}$$

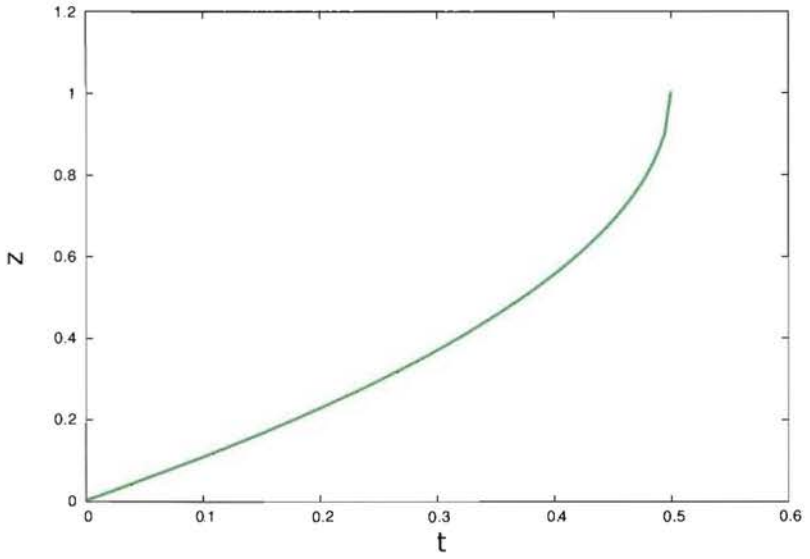

Fig. 32. Correct solution $z(t) = 1 - \sqrt{1 - 2t}$, which satisfies the initial condition $z(0) = 0$.

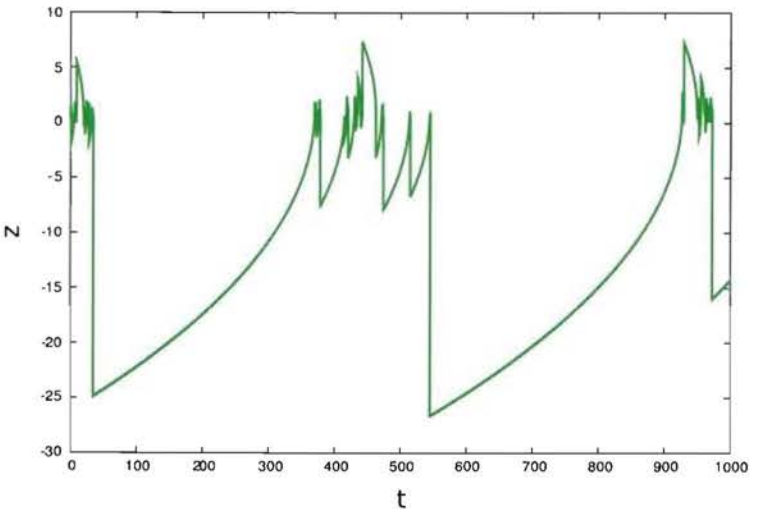

Fig. 33. Erroneous oscillation of the second-order oscillator from Fig. 31 obtained by computer-simulation via a fourth-order Runge–Kutta formula with step size $h = 0.002$ and the initial condition $z(0) = 0$.

where

$$W(\varphi) = \frac{dq(\varphi)}{d\varphi}. \tag{128}$$

From the first equation of Eq. (127), we obtain

$$v = \frac{J}{W(\varphi) - G} = \frac{d\varphi}{dt}. \tag{129}$$

Thus, Eq. (127) can be written as

$$\frac{dx}{dt} = \frac{e}{W(x) - \beta}, \tag{130}$$

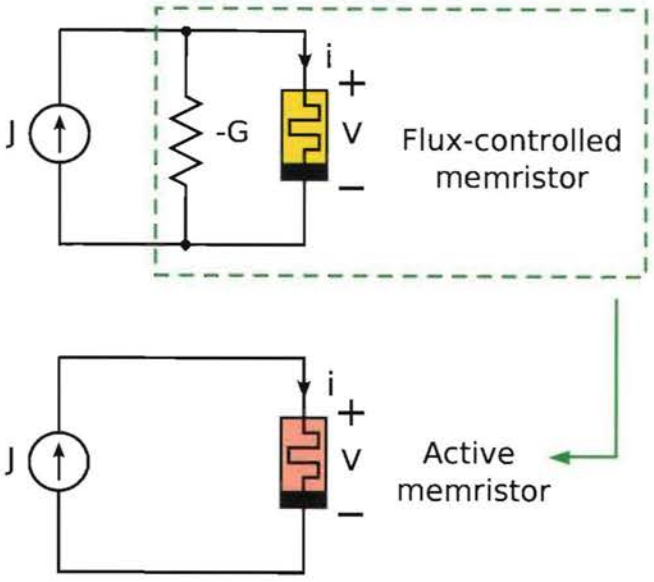

Fig. 34. A first-order oscillator with a flux-controlled memristor.

where $x = \varphi$, $e = J, \beta = G$, and the functions $q(x)$ and $W(x)$ are defined by

$$\left.\begin{aligned} q(x) &= \begin{cases} 0.05x^2, & x \geq 0, \\ 0.05x, & x < 0, \end{cases} \\ W(x) &= \frac{dq(x)}{dx} = \begin{cases} 0.1x, & x \geq 0, \\ 0.05, & x < 0. \end{cases} \end{aligned}\right\} \tag{131}$$

In this case, $q(x)$ is not a piecewise-linear function. If we set $\beta = 0.3$ and $e = 1$, our computer simulation shows that Eq. (130) exhibits an irregular oscillation as shown in Fig. 35. This computer generated solution is erroneous, and is caused by the numerical integration error at $x = 3$, since Eq. (130) can be recast into the form

$$\frac{dx}{dt} = \frac{-10}{x - 3}, \quad \text{for } x > 0, \tag{132}$$

it follows that $|dx/dt|$ tends to infinity when $x \to 3$. The exact solution of Eq. (132) is given analytically by

$$x = 3 \pm \sqrt{2(C - 10t)}, \tag{133}$$

where C is some constant, and does not exhibit any oscillations, as shown in Fig. 36. Note that solution of Eq. (133) does *not* exist for $t > C/10$, implying that a more realistic circuit model of the physical circuit is needed [Chua *et al.*, 1987].

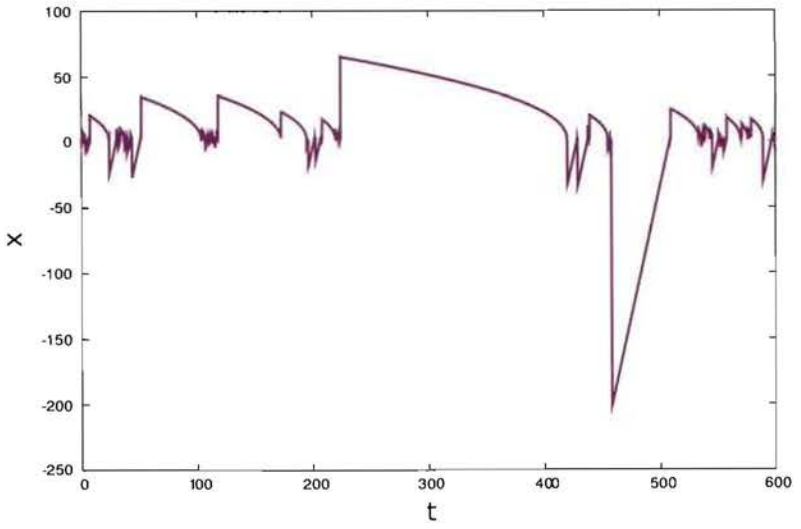

Fig. 35. Erroneous oscillation of the first-order oscillator from Fig. 34 obtained by computer-simulation via a fourth-order Runge–Kutta formula with step size $h = 0.003$ and the initial condition $x(0) = 0.3$.

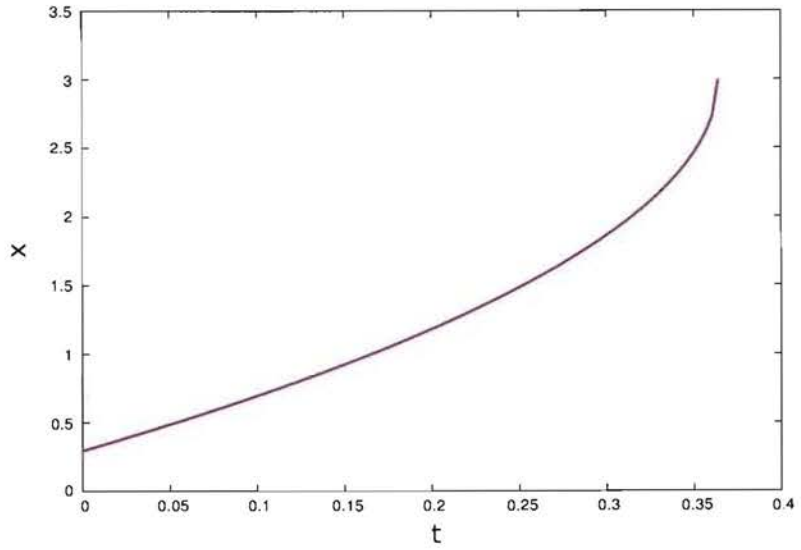

Fig. 36. Correct solution $x(t) = 3 - \sqrt{2(C - 10t)}$ $(C = 3.645)$.

5. Conclusion

We have derived several memristor-based nonlinear oscillators from Chua's oscillators. These oscillators have many interesting oscillation properties and rich nonlinear dynamics. We conclude therefore that the memristors are useful for designing nonlinear oscillators.

References

Barboza, R. & Chua, L. O. [2008] "The four-element Chua's circuit," *Int. J. Bifurcation and Chaos* **18**, 943–955.

Chua, L. O. [1969] *Introduction to Nonlinear Network Theory* (McGraw-Hill, NY).

Chua, L. O. [1971] "Memristor — the missing circuit element," *IEEE Trans. Circuit Th.* **CT-18**, 507–519.

Chua, L. O. & Kang, S. M. [1976] "Memristive devices and systems," *Proc. IEEE* **64**, 209–223.

Chua, L. O., Desoer, C. A. & Kuh, E. S. [1987] *Linear and Nonlinear Circuits* (McGraw-Hill, NY).

Chua, L. O. & Lin, G. N. [1990] "Canonical realization of Chua's circuit family," *IEEE Trans. Circuits Syst.* **37**, 885–902.

Govorukhin, V. N. [2004] "MATDS — MATLAB based program for dynamical systems investigation," http://kvm.math.rsu.ru/matds/.

Johnson, R. C. [2008] "Will memristors prove irresistible?" *EE Times* issue 1538, August 18, pp. 30–34.

Madan, R. N. [1993] *Chua's Circuit: A Paradigm for Chaos* (World Scientific, Singapore).

Strukov, D. B., Snider, G. S., Stewart, G. R. & Williams, R. S. [2008] "The missing memristor found," *Nature* **453**, 80–83.

Tour, J. M. & He, T. [2008] "The fourth element," *Nature* **453**, 42–43.